TKK Dissertations 165
Espoo 2009

PREPARATION OF POLYMERIC NANOCOMPOSITES AND THEIR STRUCTURE-PROPERTY RELATIONSHIPS

Doctoral Dissertation

Noora Ristolainen-Virtanen

Helsinki University of Technology
Faculty of Chemistry and Materials Sciences
Department of Chemistry

TKK Dissertations 165
Espoo 2009

PREPARATION OF POLYMERIC NANOCOMPOSITES AND THEIR STRUCTURE-PROPERTY RELATIONSHIPS

Doctoral Dissertation

Noora Ristolainen-Virtanen

Dissertation for the degree of Doctor of Science in Technology to be presented with due permission of the Faculty of Chemistry and Materials Sciences for public examination and debate in Auditorium KE2 (Komppa Auditorium) at Helsinki University of Technology (Espoo, Finland) on the 16th of June, 2009, at 12 n**oon.**

Helsinki University of Technology
Faculty of Chemistry and Materials Sciences
Department of Chemistry

Teknillinen korkeakoulu
Kemian ja materiaalitieteiden tiedekunta
Kemian laitos

Distribution:
Helsinki University of Technology
Faculty of Chemistry and Materials Sciences
Department of Chemistry
Laboratory of Polymer Technology
P.O. Box 6100 (Kemistintie 1)
FI - 02015 TKK
FINLAND
URL: http://polymeeri.tkk.fi/
Tel. +358-9-451 2616
Fax +358-9-451 2622
E-mail: noora.ristolainen@tkk.fi

ISBN 978-951-22-9895-2
ISBN 978-951-22-9896-9 (PDF)
ISSN 1795-2239
ISSN 1795-4584 (PDF)
URL: http://lib.tkk.fi/Diss/2009/isbn9789512298969/

TKK-DISS-2605

Multiprint Oy
Espoo 2009

ABSTRACT OF DOCTORAL DISSERTATION

HELSINKI UNIVERSITY OF TECHNOLOGY
P.O. BOX 1000, FI-02015 TKK
http://www.tkk.fi

Author Noora Ristolainen-Virtanen

Name of the dissertation

PREPARATION POLYMERIC NANOCOMPOSITES AND THEIR STRUCTURE-PROPERTY RELATIONSHIPS

Manuscript submitted 5.2.2009	Manuscript revised 4.5.2009
Date of the defence 16.6.2009	
Monograph	X Article dissertation (summary + original articles)

Faculty	Faculty of Chemistry and Materials Sciences
Department	Department of Biotechnology and Chemical Technology
Field of research	Polymer Technology
Opponent(s)	Seppo Syrjälä, D. Sc
Supervisor	Prof Jukka Seppälä
Instructor	

Abstract

Polymer nanocomposites were prepared by two different methods: (1) by melt blending polypropylene and layered clay in the presence of compatibilizers, and (2) by electrospinning poly(vinyl alcohol)/nanoclay, poly(vinyl alcohol)/nano titanium dioxide, and polyamide/nanoclay dispersions.

In this work, the preparation of PP/nanoclay composites began by exchanging the originals of natural layered clay for octadecylamine and N-methylundecenylamine. This modification yielded the desired intercalated clay structure. The ability of well-controlled stereospecific hydroxyl-functionalized polypropylene (PP-*co*-OH) compatibilizer to enable the PP-matrix to penetrate between the modified clay sheets and the properties of the resulting polymer/nanocomposite were studied. Also, a non-polar PP-based wax was tested as a compatibilizer in the composites, but the desired clay nanostructure was not achieved. The PP-*co*-OH was shown to be almost as effective a compatibilizer as the well-known maleinic anhydride-grafted polypropylene. Furthermore, addition of fire retardant particles to the melt blend improved the degree of clay exfoliation, presumably due to increased shear stress and grinding. The nanocomposites showed improved stiffness and reduced heat release rates with weakened toughness and increased moisture absorption relative to the unfilled PP or PP/clay composites.

This work also consisted of electrospinning of functional-poly(vinyl alcohol) and polyamide-6,6 with nanoclays and coated nanoscale titanium dioxide particles. The dispersions that were electrospun were prepared by two methods: by mixing the components together in a suitable solvent and by an *in situ* polymerization in the presence of nanoparticles. We were able to produce visible fiber coating depositions on substrates with uniform filler distributions along the fibers or drops. The dispersions prepared by polymerization resulted in more evenly distributed fillers along the electrospun fibers than the dispersion prepared by mixed the components together.

Keywords polymer/nanocomposites, nanoclay, functional polyolefin, electrospinning

ISBN (printed) 978-951-22-9895-2	ISSN (printed) 1795-2239
ISBN (pdf) 978-951-22-9896-9	ISSN (pdf) 1795-4584
Language English	Number of pages 60 + 58 app

Publisher TKK Dissertation

Print distribution 80

X The dissertation can be read at http://lib.tkk.fi/Diss/

VÄITÖSKIRJAN TIIVISTELMÄ	TEKNILLINEN KORKEAKOULU PL 1000, 02015 TKK http://www.tkk.fi

Tekijä Noora Ristolainen-Virtanen

Väitöskirjan nimi

Polymeeristen nanokomposiittien valmistus ja niiden rakenne-ominaisuuksien yhteydet

Käsikirjoituksen päivämäärä 5.2.2009	Korjatun käsikirjoituksen päivämäärä 4.5.2009

Väitöstilaisuuden ajankohta

Monografia	X Yhdistelmäväitöskirja (yhteenveto + erillisartikkelit)

Tiedekunta	Kemian ja materiaalitieteiden tiedekunta
Laitos	Biotekniikan ja kemian tekniikan laitos
Tutkimusala	Polymeeriteknologia
Vastaväittäjä(t)	Seppo Syrjälä, TkT
Työn valvoja	Prof. Jukka Seppälä
Työn ohjaaja	

Tiivistelmä

Polymeeriset nanokomposiitit valmistettiin kahdella eri tavalla; (1)sulatyöstämällä polypropeeni ja nanosavi kompatilibilisaattoreiden läsnä ollessa ja (2) sähkökerimällä polyvinyylialkoholi/nanosavea, polyvinyylialkoholi/nanotitaanidioksidi ja polyamidi/nanosavi dispersioita.

Tässä työssä PP/nanosavi komposiittien valmistus aloitettiin vaihtamalla alkuperäinen luonnon saven kationi oktadekyyliamiiniksi ja N-metyyliundekenyyliamiiniksi. Näin saatiin muodostettua haluttu interkaloitunut rakenne. Funktionaalisen hyvin järjestäytyneen hydroksyyli-polypropeenikopolymeeri (PP-*co*-OH) kompatibilisaattorin kykyä tunkeutua muokattujen savikerrosten väliin ja siten valmistuneen komposiitin ominaisuuksia tutkittiin. Ei-polaarista polypropeenivahaa kokeiltiin myös kompatibilisaattorina, mutta haluttua komposiitin nanorakennetta ei saavutettu. PP-*co*-OH osoitettiin olevan lähes yhtä tehokas kompatibilisaattori kuin tunnettu maleiinianhydridi-oksaskopolypropeeni. Palontorjunta-aineen lisäys sulatyöstövaiheessa edes auttoi savikerrosten irtautumista toisistaan, joka todennäköisesti vaikutti lisääntynyt leikkausvoima ja hiertyminen. Nanokomposiitit osoittivat parantavan jäykkyyttä ja pienentävän lämmön vapautumista joskin sitkeys heikkeni ja kosteuden imukyky lisääntyi verrattuna täyteaineettomaan polypropeeniin tai PP/savi-komposiittiin.

Työ sisälsi myös fuktionaalisen polyvinyylialkoholin ja polyamidi-6,6 sähkökehruun nanosaven ja päällystettyjen nanotitaanidioksidin läsnä ollessa. Dispersiot, jotka olivat sähkökerittiin, olivat valmistettu kahdella eri tavalla: sekoittamalla komponentit yhteen sopivassa liuottimessa tai *in situ* polymeroimalla nanopartikkelien läsnä ollessa. Onnistuimme tuottamaan näkyvän kuitupäällysteen alustoille ja nanopartikkelit olivat jakautuneet tasaisesti kuiduissa tai pisaroissa. Silloin kuin dispersiot olivat valmistettu polymerointimenetelmällä, niin täyteainepartikkelit olivat jakautuneet tasaisemmin kuiduissa kuin sekoitusmenetelmällä valmistetuissa kuiduissa.

Asiasanat polymeeriset nanokomposiitit, nanosavi, funktionaaliset polyolefiinit, elektrospinning

ISBN (painettu) 978-951-22-9895-2	ISSN (painettu) 1795-2239
ISBN (pdf) 978-951-22-9896-9	ISSN (pdf) 1795-4584
Kieli Englanti	Sivumäärä 60 + 58 liitteet

Julkaisija TKK Dissertation series

Painetun väitöskirjan jakelu 80

X Luettavissa verkossa osoitteessa http://lib.tkk.fi/Diss/

PREFACE

The experimental work for this thesis was carried out between 2002 and 2006 in the Department of Biotechnology and Chemical Technology at the Helsinki University of Technology. The work consists of several projects, which were partly funded by the National Technology Agency (TEKES) and the Research Foundation of the Helsinki University of Technology.

I wish to express my gratitude to Prof. Jukka Seppälä for giving me the opportunity to work with him and with his research group. I would like to thank Dr. Barbro Löfgren for her guidance and Prof. Ali Harlin for introducing me to electrospinning.

I am grateful to my co-authors for their contributions and valuable comments. I, especially owe my thanks to Dr. Ulla Hippi, Dr. Pirjo Heikkilä, and Ulla Vainio. I would like to thank Dr. Santeri Paavola for synthesizing functional-polypropylenes for me. I would also like to thank Tapio Saarinen for providing guidance in rheology. Piia Haimi is thanked for her assistance in the studies we did together. I owe my deepest thanks to the Laboratory of Polymer Technology for providing a pleasant working atmosphere and support.

Most of all, I would like to thank my parents, Paula and Eero†, and my brother Tero and his wife Laura for their loving support. Special thanks are given to my supporting friends: Anna, Minna, and Mira, who have “lent me their ears”. Finally, I would like to thank Sami for being there for me.

LIST OF PUBLICATIOS

This thesis is based on the following five appended publications:

Ristolainen, N., Vainio, U., Paavola, S., Torkkeli, M., Serimaa, R., Seppälä, J., Polypropylene/organoclay nanocomposites compatibilized with hydroxyl-functional polypropylene, *J. Pol. Sci, Part B; Pol. Phys*., **43**, 14 (2005) 1892-1903.

Ristolainen, N., Hippi, U., Seppälä, J., Nykänen, A., Ruokolainen, J. Properties of polypropylene/aluminum trihydroxide composites containing nanosized organoclay, *Pol. Eng. Sci*., **45**, 12 (2005) 1568-1575.

Ristolainen, N., Heikkilä, P., Harlin, A., Seppälä, J., Poly(vinyl alcohol) and Polyamide-66 Nanocomposites Prepared by Electrospinning, *Macromol. Mat. Eng*., **291** (2006) 114-121.

Hippi, U., Ristolainen, N., Löfgren, B., Seppälä, J., Metallocene Catalyzed Functional Polyolefins in Composites, *Polyolefin Composites*, Ed. Domasius Nwabunma, Thein Kyu, Chapter 8, (2007) 207-227.

Ristolainen, N., Heikkilä, P., Harlin, A., Seppälä, J., Electrospun nanofibers prepared by two methods: *in situ* emulsion polymerized PVA/nanoTiO_2 and mixing of functional-PVA with nanoTiO_2, *Autex RJ*. **8**, 2 (2008) 35-40.

The author's contributions to the appended publications are as follows:

Publication I, II and IV: I was, in cooperation with Ulla Hippi, responsible for the research plan. I selected the components, carried out preparation of the PP/nanoclay composites and characterized the properties thereof, with the exception that Santeri Paavola synthesized and characterized the novel compatibilizer, and X-ray measurement and analysis was carried out mostly by Ulla Vainio. The manuscripts were prepared together with co-authors.

Publications III and V: I planned, selected fillers, and carried out the preparation of the polymer/nanofiller dispersions. Pirjo Heikkilä is responsible for the electrospinning. I contributed to the characterization of the coated surfaces. The manuscripts were prepared together with the co-authors.

CONTENTS

ABBREVIATIONS

ATH	Aluminum trihydroxide
ATH (SA)	Stearic acid-coated aluminum trihydroxide
ATRP	Atomic transfer radical polymerization
DSC	Differential scanning calorimeter
FESEM	Field emission scanning electron microscope
HRR	Heat release rate
MWD	Molecular weight distribution
nanoTiO_2	Nanoscale titanium dioxide
NMR	Nuclear magnetic resonance spectroscopy
Organoclay	Natural montmorillonite clay with quaternary ammonium salt
Organoclay11	Natural montmorillonite clay with N-methylundecenylamine
Organoclay18	Natural montmorillonite clay with octadecylamine
PA66	Polyamide-6,6
PP	Polypropylene
PP-*co*-OH	Polypropylene/10-undecen-1-ol- copolymer
PP-*g*-MA	Maleinic anhydride-grafted polypropylene
PPwax	Polypropylene-based wax
PVA	Poly(vinyl alcohol)
PVAc	Poly(vinyl acetate)
RAFT	Reversible-addition fragmentation chain transfer
SAXS	Small-angle X-ray
SEM	Scanning electron microscope
TEM	Transmission electron microscope
UV	Ultraviolet light
WAXS	Wide-angle X-ray
WVT	Water vapor transmission rate

SYMBOLS

α	Alpha crystalline structure of PP
β	Beta crystalline structure of PP
ε	Elongation at break (%)
σ	Tensile stress (MPa)
c	Solubility (mol/ cm^3 x 10^{-6})
D	Oxygen diffusion coefficient (cm^2/s x 10^{-7})
E	Tensile modulus (MPa)
P	Permeability (g/ms x 10^{-9})
wt-%	Weight percentage
Å	Angstrom
q	Distance (1/Å)

1 INTRODUCTION

1.1 General background on polymer/nanofiller composites

Fillers are typically used to enhance specific properties of polymers [1] and the polymer/nanocomposites based on nanoclays have gained attention due to their ability to improve mechanical, [2 - 5] thermal, [6 , 7] barrier, [8 , 9] and fire retardant [10 - 14] properties of polymers. Polymer/nanocomposites have been shown at lower[15,16] or equal loadings to have properties that are equal or better than those of polymer composites with conventional filler.[17-22] The nanofillers featuring antibacterial properties, like nanoscale titanium- and silver-based particles, could be applicable in filtration, hygiene and hospital disposables applications, or in consumer products.

Nanosized fillers have been introduced in a wide spectrum of applications ranging from providing photo-catalyst activation [23] and conductivity [24 , 25] to improving melt processability[16,26-28] and moisture barrier properties.[29] The special properties of nanoparticles are due to their size and high relative surface area to volume ratio. The optical clarity of a spherical nanosize particle is better than that of its equivalent conventional-size filler, because the diameter is smaller than the wavelengths of light. As a nanosize filler particle has a larger specific surface area than its analogous traditional-size filler particle, it interacts more with its surroundings.[1] Thermodynamic stability of the polymer nanocomposite, which is due to the large interfacial phase between the matrix and the nanoparticle[15], yields the physical properties of the composite.

A polymer/nanocomposite can be defined as a polymer-nanofiller system in which the inorganic filler is on a nanometric scale at least in one dimension and it can be a polymer/nanoparticle blend or a hybrid. The composite interconnection can be based on a secondary force or physical entanglement.[30,31] The polymer/nanofiller-hybrid, in turn, is formed when the polymer and the nanoparticle are covalently bonded. The covalent bond can be formed during the *in situ* polymerization (the monomer or the growing polymer chain can react with the filler particle), or during the composite processing.

Uniform filler distribution in the polymer matrix is desired. It can be a challenge to create a favorable interaction between the polymer and the nanofiller and thus avoid phase separation and agglomeration of the filler particles. An example is the natural layered clay; it delaminates completely in water and in some polar polymer melts or solutions like in polyamide, but it does not spontaneously disperse in non-polar polyolefin melts like polypropylene melt. Two possible options for improving compatibility of the components will be examined here: chemically modifying one, or more of the components or introducing a suitable compatibilizer.

1.2 Nanoparticles of the polymer composites

Nanoparticles exist inspherical, tube and whisker, and plate-like shapes and at least one of the three dimensions is required to be on a nanometric scale. Nanostructures of layered clays are further categorized as *intercalated*, where the polymer chains have penetrated between the clay layers in a well-ordered multilayer morphology, and *exfoliated*, where the clay layers have dispersed along the matrix and have no organized structure. [32] Carbon nanotubes also exhibit two nanostructures, single-walled tube, *SWNT*, and multi-walled carbon nanotube, *MWNT*, which is composed of several tubes within each other.

Nanoparticles, like the conventional filler particles, can be prepared by breaking up a large particle (nanoclays and other minerals) or by building them from bottom up (carbon nanotubes and metal oxides). Regardless of the preparation method, it is important to inhibit agglomeration of the nanoparticles and ensure good adhesion to the matrix.[1] It is possible to coat or surface-treat the nanosize particles[33-35] as done with microsize particles.[36] A wide spectrum of polar agents, such as silanes and polyalcohols, and non-polar agents, such as stearic acid and fatty acids, are commercially available coating agents for inorganic particles[1]. In contrast, layered nanoclays[37-39] and carbon nanotubes are surface.

Surface treatment of nanoclays, which typically involves cation exchange, promotes delamination of the clay sheets in the matrix.[1,] The cation, or alternatively the intercalated media between the clay layers, determines the interlayer space, the *gallery*, and the cation exchange capacity.[15,40- 43] Alkyl amines are one group of cations used to replace the original cations of natural clay, because they can be easily tailored by changing the length and number of the alkyl tails[44,45] and they favor attraction of hydrocarbons like polyolefins. The modification of natural clays towards an organophilic nature is called *organomodification*.

1.3 Functionalized polymer with nanoparticles

Polymers are utilized in various different applications based on their properties; polypropylene is used for its mechanical strength in consumer packages, poly(vinyl alcohol) is widely used for its water solubility and transparency in film applications on various paper and textile surfaces, and polyamide, in turn, is used for its good dimensional stability and chemical resistance in yarn applications. [46]

Changes in a polymer's structure can have a dramatic effect on its behavior, which is not always desired. Structure-property relationships can be illustrated by the following two examples: the solubility of poly(vinyl alcohol) is influenced by the degree of hydrolysis[47] and the moisture resistance of polyamide is dependent on the number of carbon atoms of the monomer used.[46] The structure of a polymer can be modified by introducing functional groups to the polymer backbone and/or to the side chains[46, 48-53] in various ways such as grafting[54] and using various different monomers in the polymerization reaction.[55] However, unwanted cross-linking and polymer degradation reactions can also be observed when post-modifying by melt free radical grafting, which could be avoided by using polymerization techniques such as atomic transfer radical polymerization (ATRP)[56] and reversible-addition fragmentation chain transfer (RAFT).[35] These by, for example, offer intriguing new possibilities to produce the polymers and thereby polymer nanocomposites such as initiating polymerization on the hydroxyl groups on the surface of a clay sheet. The monomers could be styrene, methyl methacrylate, or vinyl acetate.[32,57,58] In addition, developments in catalyst technology[59,60] such as metallocene polyolefin polymerizations enable production of an excellent controlled comonomer distribution and stereospecificity along the polymer backbone or chain end.[61,62]

If chemical treatment of the matrix polymer or the filler needs to be avoided or the interaction between the components is insufficient, a third component, such as polymer compatibilizer[63 - 65], can be added to the composite. Compatibilizers are added especially to polyolefin/nanoclay composites prepared by melt blending, because the organomodification of the clay is seldom sufficient to create a favorable interaction between polymer chains and the clay sheets.[2, 66 - 69] The interfacial adhesion between the compatibilizer and the clay galleries is influenced by the functionality and its concentration, the molecular weight and the molecular weight distribution (MWD) of the compatibilizer, and the mass ratio of the compatibilizer to the clay.[41,70]

1.4 Preparation of polymer/nanofiller composites – especially by the electrospinning technique

Preparation methods for polymer/nanocomposites can be the same as for traditional polymer composites, for example they can be prepared by blending the components together or by *in situ* polymerization in the presence of a (nano)particle. The blending can be carried out either in a polymer melt, if the components tolerate the blending temperature above the melting temperature of the polymer,[48,71,72,] or in a polymer solution, if a suitable solvent is available.[73,74,75] *In situ*

polymerization in the presence of the nanoparticle is possible in all different polymerizations,[76,77] but only if the nanoparticle does not inhibit the polymerization reaction. Regardless of the preparation method of the polymer nanocomposite, a good compatibility between the components is essential in order to produce a homogenous polymer nanocomposite.[78,79,80] Compatibility can be improved by selecting suitable external blending conditions, such as by adjusting the temperature and the mixing intensity,[52] or by chemical modifications of the filler and/or the polymer, as mentioned earlier.

In addition, electrospinning is a unique technique for producing polymer nanofibers(/drops) with nanofillers. It is a promising method for producing an extremely light weight coating, where nanoscale polymer fibers with a large specific area[81] are produced on a substrate from a polymer melt, solution, or dispersion.[82] The nanoparticle functionalities are incorporated into the fibers, as with fillers in polymers that reinforce or increase the electrical conductivity of the fibers.

Every polymer solution and dispersion has a unique fiber-forming limit, above which a continuous fiber network is obtained. The solvent evaporates from the polymer dispersion jet as it travels to the substrate in electrospinning, and a polymer nanofiber or -drop nanocomposite deposits on the substrate. A non-miscible third component can be used to encapsulate the filler in emulsion drops during travel.[83,84] It must evaporate during the travel from the electrode to the substrate.

The polymer solution[85] and dispersion[86] properties influence the electrospun polymer/nanoparticle fiber and network formation. Bead-like polymeric structures may appear, but the distance between them lengthens as the viscosity of the pre-spun solution or dispersion increases.[87,88] The fiber diameter, the network structure, and the filler distribution along the fibers can be controlled by modifying the dispersion properties, such as the molecular weight of the polymer,[89-91] the interactions between the components,[92,93] and the concentration of the polymer and the filler in the dispersion,[94-96] and the processing parameters, such as the voltage between electrodes and their distance[97,98] and the feeding rate.[99] Filler particle agglomerates can disturb the flow of a spinning dispersion and the formation of a continuous jet.

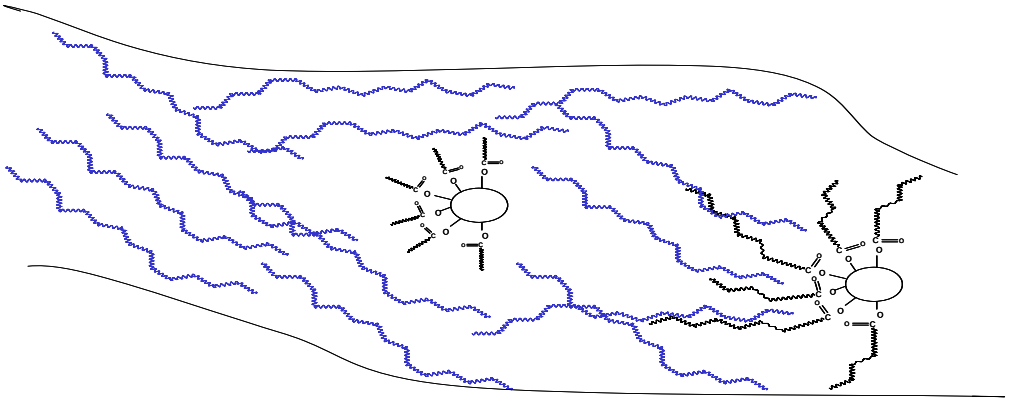

Figure 1. Schematic image illustrates the influence on compatibility of chemically modified filler particles and polymer chains.

1.5 Scope of the study

The compatibility between polymer matrix and filler particles has been studied in the Laboratory of Polymer Technology at Helsinki University of Technology. The target of this present work was to prepare polymer/nanocomposites by melt blending polypropylene (PP) with nanoclay and by electrospinning poly(vinyl alcohol) (PVA) and polyamide-6,6 (PA66) with nanoclay or nanosize titanium dioxide and studying their properties. The thesis summarizes the research reported in five publications and some unpublished data.

The objective of the first part of the work was to study the relationship between the structures of the nanoclay and the resulting PP/nanoclay composites. The influence of the functionality and its concentration, the molecular weight, and molecular weight distribution of the polymer compatibilizer were especially of interest. In addition, the relationship between morphology, flame retardancy, and thermal, mechanical, and barrier properties and the structure of the polymer/clay nanocomposite was investigated in this work. The compatibilizer/clay ratio and the resulting exfoliation rate of the clay was studied as well.

The first challenge was to intercalate the hydroxyl-functional polypropylene compatibilizer (PP-*co*-OH) between clay sheets and thus create a good interfacial interaction between the polypropylene matrix (PP), the compatibilizer, and the clay galleries. The emphasis in publication I was to prepare and retain the nanostructure of the clay after melt blending. Here, the natural clay was rendered more organic in nature by two different alkyl ammonium cations. A novel amine, N-methylundecenylamine, was prepared especially for this study. The ability of hydroxyl-functionalized polypropylene to penetrate into the clay galleries was studied. The aim was to replace maleinic anhydride-grafted polypropylene with PP-*co*-OH in the PP/nanoclay composites.

The morphology, thermal and mechanical properties (tensile and impact properties), and flame retardant properties of PP/nanoclay composites were studied and are reported in publications II and IV. It was intriguing to study the synergy of a conventional-size inorganic flame retardant particle, aluminum trihydroxide (ATH), and the nanoclay in flame retardancy tests and the influence of the ATH on the degree of clay exfoliation in the melt blending. In addition, a non-polar PP-based wax, which is actually a swelling agent for an organomodified clay, was also used as a compatibilizer in the PP/nanoclay composites in analogous studies. This data is not published in scientific journals.

The next step was to explore the knowledge gained. Therefore, polymer/nanoclay composites were prepared for a completely different application field: coatings on paper. As attention was turned to the development of polymer/nanofiller dispersion for the electrospinning technique in coating applications, the polypropylene matrix was changed to poly(vinyl alcohol) (PVA) and polyamide-6,6 (PA66). The results are covered in publication III. The electrospun dispersions were prepared in two ways: 1) blending the components together and 2) *in situ* polymerization in the presence of nanoclay in suitable solvents. The main goal was to produce a visible coating area on a substrate. The influence of the two preparation methods on the filler distribution along the fibers and the fiber networks were studied. The filler carrying-ability was enhanced by carboxyl- and silanol-groups on the PVA.

Finally, attention was turned to electrospinning of PVA with nanoscale titanium dioxide (nanoTiO_2) and especially of interest was the dispersion of the filler particles along the fibers. This work is reported in publication V. The dispersion preparations were analogous to those for the nanoclay dispersions. In this study, the influence of three hydrophilic coating agents for the nanoTiO_2 on the distribution of the nanoTiO_2 along the electrospun fibers was studied. In addition, the hydroscopicity of the coated substrates was tested.

2 EXPERIMENTAL

2.1 Materials

The composites were prepared from range of polymer matrices and compatibilizers, both commercial and synthesized in the Department of Biotechnology and Chemical Technology (Table 1). The matrices were: extrusion and injection mold grade polypropylene (PP), polyamide 6,6 (PA66), and four different poly(vinyl alcohol)s (PVA). Two grades of polypropylene (PP) were used as matrix: neat (HE 125 MO) and a film extrusion grade (HC205TF), both from Borealis Polymers. Commercial compatibilizers were polypropylene nanocomposites: maleic anhydride-grafted polypropylene (PP-*g*-MA) (BB125E) with a functionality content of 0.5 wt-% was from Borealis Polymers, and polypropylene wax (TP LICOCENE PP 6102 Fine grain) was from Clariant. Three commercial PVA grades from Kuraray Specialities Europe were used: neat PVA, Mowiol 28-99, a fully hydrolysed polymer (99.4 mol-%) with a viscosity of 28 ± 2cP (20°C and 4 wt% solution), abbreviated n-PVA; anionic charged PVA, KL-318 modified PVCA with carboxylic groups with a degree of hydrolysis 85-90, DP 1750, with a viscosity of 20-30cP (20°C and 4wt% solution), abbreviated a-PVA; and functionalized non-charged PVA, R1130 with silanol groups, DH 98-9, with a viscosity of 20-30cP (20°C and 4 wt% solution), abbreviate f-PVA. Commercial PA66, abbreviated as c-PA, was obtained from Fluka, and the formic acid was from Bang & Co. In addition, polyamide 6,6 s-PA66 and poly(vinyl alcohol)s s-PVA were synthesized. The vinyl acetate monomer was from Aldrich, the $K_2S_2O_8$ initiator from Merck, and the sodium dodecyl sulfate emulsifier from Fluka. The two terminators were hydroquinone from Fluka and NaCl from Aldrich. The methanol used in alcoholysis of PVAc was from Merck. 1,6-Diaminohexane, dichloromethane, and adipoyl chloride for synthesis of PA were from Fluka and NaOH from Merck. Aqueous acetic acid for rinsing was from Merck. The pH of the solutions was adjusted with HCl from Riedel-de Haën.

The commercial compatibilizers used were maleic anhydride-grafted polypropylene (PP-*g*-MA) and polypropylene wax (PPwax), and the hydroxyl-functionalized polypropylene (PP-*co*-OH) was synthesized in the Department of Biotechnology and Chemical Technology. The synthesis is reported elsewhere.[100]

Table 1. The polypropylene, poly(vinyl alcohol), and polyamide used in this study.

Abbreviation	Purpose	Grade	Supplier	Publication
PP	Matrix	HE 125 MO	Borealis Polymers	I, II, IV
PP	Matrix	HC205TF	Borealis Polymers	-
PP-*g*-MA	Compatibilizer	BB125E	Borealis Polymers	I, II, IV
PP-*co*-OH	Compatibilizer	synthesized	Dept. Biotech. and chemical tech.	I, II, IV
PPwax	Compatibilizer	TP LICOCENE PP 6102 Fine grain	Clariant	-
n-PVA	Matrix	Mowiol 28-99	Kuraray Specialities Europe	III, V
a-PVA	Matrix	KL-318	Kuraray Specialities Europe	III, V
f-PVA	Matrix	R1130	Kuraray Specialities Europe	III, V
u-PVA	Matrix	laboratory grade	Merck	-
s-PVA	Matrix	synthesized	Dept. Biotech. and chemical tech.	III
PA	Matrix	PA66	Fluka	III
s-PA	Matrix	synthesized	Dept. Biotech. and chemical tech.	III

Two different types of nanosized fillers were used as well as a traditional filler with and without stearic acid coating (Table 2). The nanofillers included two types of clays and three differently coated titanium dioxides. The unmodified montmorillonite (Cloisite®Na^+), with a cationic exchange capacity of 94 meq/100 g montmorillonite, from here on referred as clay, and sodium montmorillonite organomodified with a quaternary ammonium salt (Cloisite®15) with a cationic exchange capacity of 125 meq/100 g montmorillonite, abbreviated as organoclay, were from Southern Clay Products, Inc. Three nanoTiO_2 grades were obtained from Kemira Pigments: M212®, coated with trimethylolpropane, abbreviated TiO_2 (oh); M111®, coated with alumina, abbreviated TiO_2 (al); and L181®, coated with glycerol, abbreviated TiO_2 (gl). The two conventional-size fillers were stearic acid (SA) coated (Apyral® 60E) and untreated (Apyral® 60D) aluminum trihydroxides (ATH). They were from Nabaltec (publication II).

Table 2. The nanosized clay and TiO_2 fillers used in this study.

Abbreviation	Type	Grade	Supplier	Publication
clay	natural clay	Cloisite®Na^+	Southern Clay Products, Inc	I, III
Organoclay11	cation exchange		Dept. Biotech. and chemical tech.	I, IV
Organoclay18	cation exchange		Dept. Biotech. and chemical tech.	I, IV
Organoclay	quaternary ammonium salt	Cloisite®15	Southern Clay Products, Inc	II, III, IV
nanoTiO_2 (oh)	coated with trimethylolpropane	M212®	Kemira Pigments	V
nanoTiO_2 (al)	coated with alumina	M111®	Kemira Pigments	V
nanoTiO_2 (gl)	coated with glycerol	L181®	Kemira Pigments	V

Polymer nanofiller dispersions were electrospun onto three different substrates. Black nonwoven fabric composed of cellulose-based fiber and polymer binders with a grammage of 50 g/m^2 was used in studies of morphology of the fiber network and filler distribution. Colored paper was used in coating studies where visual appearance (shape, size and evenness of the coating) was important. White paper was used in samples for measurements of coating properties.

2.2 Organomodification of natural clay

The natural clay was treated to render it more organophilic in nature. Octadecylamine (3.11 g) or N-methylundecenylamine (2.131 g) and conc. HCl (1.5 ml) were dispersed into water (100 ml) at 80°C with stirring to yield white foam. The aforementioned mixture was added to a mixture of clay (8.0 g) and water (400 ml) and it was vigorously stirred for 15 min. The precipitate was collected, washed with water, and dried at 80˚C for 3 h. Octadecylamine-modified organoclay is abbreviated as organoclay18 and the N-methylundecenylamine-modified organoclay as organoclay11.

2.3 Melt blending and injection molding of PP/nanoclay composites

Two different melt blending extruders were used to prepare the PP-based nanocomposites. The PP-based clay nanocomposites were, by weight of PP/compatibilizer/clay, 90/5/5 and 70/20/10. The PP/ATH composites consisted of 70 wt-% of polypropylene with 30 wt-% ATH. The amount of compatibilizer added was 10 wt-%, which was subtracted from the polypropylene phase, and the amount of organoclay was 5 wt-%, which was subtracted from the ATH phase. When extrusion PP grade was used instead of the injection molding grade, the composites' ratios (PP/compatibilizer/organoclay) were 70/20/10, 80/10/10, 85/10/5, 90/5/5, 91/6/3, and 94/3/3.

The components were mixed in a container before the melt blending. All except the extrusion PP grade-based composites were prepared with a co-rotating twin-screw midi extruder (DSM) with a capacity of 16 cm^3, a screw length of 150 mm and a screw speed of 60 rpm. The temperature of the extrusion and injection molding was 200˚C. The melt blending time was 15 min. The composites were injection molded into tensile and impact test specimens with a mini-injection molding machine (DSM). The temperature of the mold was 80˚C.

The extrusion PP grade-based composites were prepared with a co-rotating Brabender Plasti-Corder PLE 651 with a DSK 42/7 twin-screw extruder and a screw speed of 65 rpm. The temperature of the extrusion was 200˚C. The process was continuous. The extrudate was pelletized and the composites were injection molded into tensile test specimens with an injection-molding machine ENGEL ES 200/40 at 200°C. The temperature of the mold was 23˚C.

2.4 In situ polymer synthesis of PVA and PA66 in the presence of nanofiller

Emulsion polymerizations of vinyl acetate monomer in the presence of the nanoparticles were carried out in a 1 dm^3 batch reactor. 10 g of clay or nanoTiO_2 was dispersed in water in the reactor, and 100 g of distilled vinyl acetate monomer was added to the reactor under argon atmosphere. 1 wt-% of emulsifier (sodium dodecyl sulfate) and 0.15 wt-% initiator ($K_2S_2O_8$) were added to the solution at 50°C. The polymerization was terminated with an aqueous solution of hydroquinone and NaCl. The PVAc was washed with warm water and, after drying, was added to methanol with continuous stirring. Soxhlet extraction with methanol was carried out to remove residues.

PA66 was synthesized in the presence of natural clay or orgnanomodified clay at room temperature. The organic phase consisted of 900 ml dichloromethane and 12.0 ml adipoyl chloride and the synthesis was accomplished by adding a water phase (600 ml), which contained 2 g of clay dispersed in water and a mixture of 4.3 g NaOH and 6.3 g diaminohexane. Stabilization was accomplished with aqueous acetic acid (10 wt-%), the product was washed thoroughly with water and dried overnight. A similar synthesis was carried out by adding 2 g organoclay to the organic phase.

2.5 Preparation of PVA and PA66 with nanofiller dispersions

Commercial PVA and PA66 nanofiller dispersions were prepared by dispersing PVA-based composites in water and PA66-based composites in formic acid. The PVAs and PA66 are presented in Table 1. A wide range of dispersions were prepared in which the composition concentrations varied as shown in Table 3. In addition, a summary of the influence of pH on PVA-based dispersions, and feeding order of the PVA- and PA66-based dispersions, is presented in the same table.

Table 3. Concentration percentages (wt%) of PVA and PA66 with nanoparticles in the electrospun dispersions

Study\Materials	Solvent	PVA	PA66	clay	nano$Ti0_2$
pH 9-10	90	8		2	
pH 1-2	90	8		2	
Feeding A PVA	89	10		1	
Feeding B PVA	89	10		1	
Feeding A PA66	89		10	1	
Feeding B PA66	89		10	1	
PVA/nano$Ti0_2$	90	9			1

In the pH study, the original pH of the PVA/nanoclay solution in water was changed from alkaline to acidic. The pH of PVA with organomodified nanoclay is 9-10. Acidic conditions (pH 1-2) were achieved with the addition of HCl.

In the feeding order study of PVA-based solutions, the solutions contained water/functional PVA/nanoclay in a ratio of 89/10/1 wt-% (the ratio between the polymer and the filler was 10:1). In the first series (A), the polymer was dissolved in water before addition of the montmorillonite. In the second series (B), the feeding order was the reverse: the montmorillonite was swelled in water before addition of the polymer. Preparation of the two PVA series was carried out at *ca*. 80°C with stirring for 3 hours. A similar feeding order study was carried out withPA66. In the A series for PA66, the PA (10.0 g) was dissolved in formic acid (89.0 g) and either clay or organoclay (1.0 g) was added to the solution and stirred for 30 min. In the B series the order was reversed.

In the first study the non- treated and silanol- and carboxylic- functional PVAs were prepared by dissolving the PVAs in water at *ca*. 80°C and mixing for 3 h. NanoTiO_2 was added to the viscous PVA solution with stirring. The dispersions contained water/PVA/nanoTiO_2 in a ratio of 45:4.5:1. In the second study only u-PVA was dissolved in water at *ca.* 80 °C and mixed for 2 h.

NanoTiO$_2$ (oh) was added to the u-PVA solution with stirring. The solutions contained water/u-PVA/nanoTiO$_2$ (oh) in rations of 88.8/7.6/3.6 and 90.3/7.2/2.5.

2.6 Characterization of synthesized polymers

The molecular weights and molecular weight distributions of the PVAc for PVA/TiO$_2$ dispersions were determined with a Waters 717 plus autosampler gel permeation chromatograph operating at room temperature, with tetrahydrofuran used as eluent.

The molecular weights and molecular weight distributions of the PP-*co*-OH compatibilizers were determined with a Waters Alliance GPCV 2000 gel permeation chromatograph operating at 140°C, with 1,2,4-trichlorobenzene used as eluent. Melting temperatures (T_m) and enthalpies (ΔH_m) were determined with a Mettler Toledo DSC 821^e differential scanning calorimeter (DSC) upon reheating of the polymer sample up to 190°C at a heating rate of 10 °C/min. The ^{1}H NMR spectra were recorded on a Varian Gemini 2000 300 MHz spectrometer at 120°C from samples dissolved in 1,1,2,2-tetrachloroethane-d_2.

2.7 Electrospinning of polymer nanoparticle dispersions

Polymer solutions of PVA and PA66 with clays and nanoTiO$_2$ were prepared for a wide range of studies. Viscosities of all dispersions were measured before the electrospinning with a Brookfield viscometer, at room temperature. The feeding rate of the solution was determined by gravity. The syringe needles inner diameters varied from 0.8 to 0.16 mm and the capillary lengths from 27 mm to 50 mm. The needles, the distance between the needle and the collector, and the voltages were adjusted for every dispersion separately. The equipment is described in more detail in the Doctoral Thesis of Pirjo Heikkilä.[101]

Viscosity is one of the main factors influencing fiber formation in electrospinning because it determines the formation of the electrospun fiber and the network structure. It is relatively easy to change viscosity by 1) changing the concentration of the filler and polymer, 2) changing the feeding order of the components during the mixing, 3) changing the pH of the solution, and 4) tailoring the interactions between the components by functionalizing the components in the solution.

2.8 Characterization of polymer nanocomposites and dispersions

The distance between the clay sheets was measured with small-angle x-ray scattering (SAXS) and wide-angle x-ray scattering (WAXS) from the injection-molded samples with perpendicular transmission geometry. Radiation from a sealed anode x-ray tube with a Cu anode in point focus was monochromatized with a nickel filter and a totally reflecting mirror to give CuKα radiation (λ = 1.54 Å). In the SAXS setup, the sample-to-detector distance was 19 cm and in the WAXS setup 6 cm, covering in total a *q*-range from 0.06 to 2.35 $Å^{-1}$. The scattering vector is defined as $q = 4\pi\sin(\theta)/\lambda$, where 2θ is the scattering angle. The scattering was detected on an HI-Star area detector (Bruker AXS) and one-dimensional scattering curves were obtained by integrating over the azimuth angle 2π. The intensities were corrected for absorption and a geometrical correction was applied to the WAXS intensities to correct for the flatness of the detector. The intensities were integrated, the absorption was corrected, and the background caused by air scattering was subtracted. The scattering angle calibration was done using silver behenate d = 58.373 Å.[102]

The fractured surfaces and fiber morphology were investigated with a JEOL JSM-6335F field emission scanning electron microscope (FESEM). Before fracturing, the samples were cooled in liquid nitrogen. The fractured samples were sputter-coated with chromium under argon. The electron micrographs were recorded using an acceleration voltage of 5.0 kV. The fiber diameter and morphology was measured from JEOL JSM-T100 SEM images with ImageTool 3.0 with at least 100 measurements per sample.

Ultra-thin sections of the organoclay samples, approximately 70 nm in size, were wet-cryomicrotomed at –40˚C in a 50%/50% mixture of diethyl sulfoxide (Fluka 99%) and distilled water as boat fluid. The sections were laid on 600 mesh-copper grids for study with a Tecnai 12 transmission electron microscope (TEM).

Melting and crystallization behavior were measured with a Mettler Toledo DSC821^e differential scanning calorimeter (DSC) under nitrogen. The cooling and reheating rates were 10 ˚C/min and the temperature range was from 0˚C to 180˚C.

Melt viscosities were carried out with a Rheometric Scientific SR-500 stress-controlled rotational rheometer and capillary rheometry. The aforementioned measurements were carried out on compression-molded disks at 210°C under nitrogen atmosphere. Frequency sweeps, which were needed to locate the linear viscoelastic region, were performed following the stress sweeps. The measurement geometry was plate and plate. Capillary rheometry, using a Göttfert

Rheograph 2002, was used to measure the shear stress and shear rate of the materials at a given temperature with applied pressure. The radius of the capillary was 1 mm, and length of the die used was 40 mm. The chamber holds 200 g of composite material. Experiments were run at 200°C with piston speeds that had a range from $8.680 \cdot 10^{-3}$ mm/s to $7.638 \cdot 10^{-1}$ mm/s. These speeds corresponds to pressures from ~0.5 to 150 bar. The shear stresses that are calculated by the system assume that the capillary is infinitely long and no edge effects occur.

Before the mechanical tests, the injection-molded samples were conditioned at 23˚C with a relative humidity of 50% for 4 days. The tensile tests were carried out with an Instron 4204 universal testing machine with a test speed of 2mm/min or 10 mm/min with a specimen-type 1BA according to the standard ISO 527-1993(E). Charpy impact tests of unnotched and notched specimens with dimensions of 4 x 6 x 50 mm were made with a Zwick 5102 pendulum-type testing machine according to ISO 179-1993(E).

The water vapor transition rate (WVT) was measured according to standard EN 96 using a desiccant method. The measurements were carried out in a test chamber with saturated KCl solution. The solution was stirred continuously. In this way the humidity in the chamber was kept at a constant 86% at room temperature (22°C).[103] The films were first hot-pressed as thin films and the thickness varied between 0.12 mm and 0.17 mm. Silica was added to the test cups to keep the air dry inside the cup. The films were then mounted on the cups with melted wax. The diameter of the film area was 8.2 cm. The tests carried out over a period of four weeks and the weights of the samples were measured twice a week. All the sample ratios were 90/5/5.

The oxygen solubility was measured with a membrane/electrode combination, in which the polymer composite membranes were coated with platinum at 20°C. The membranes were applied at 150 kN pressure for 60 seconds at 140 °C before coating with a 0.5 mg/cm^2 platinum layer. The working electrode was a platinum microelectrode (diameter 50 μm), which was mounted in a glass barrel.

The flammability properties of the composites were measured with a cone calorimeter under a heat flux of 35 kW/m^2 according to ISO 5660-2002 (E). The size of the samples was 80 mm x 80 mm x 3 mm.

Ink penetration was tested for selected samples with IGT REPROTEST AIC2-5 according to SCAN-P 36:02 and SCAN-P 86:02 methods.

The surface energies of PVA/nanoTiO_2-coated paper samples were determined by using a goniometric system, which is based on contact angle measurements. Ten drops of three

different liquids, water, formamide, and hexadecane, are dropped onto the surface of the sample. The operation is recorded on film, and pictures of the droplets in equilibrium are saved in digital mode. The contact angles were determined from the images and the surface energies were calculated from contact angles based on the geometric mean (Kaeble method).

3 SUMMARY OF RESULTS

The polypropylene-based (PP) composites were prepared by melt blending and injection molding, while poly(vinyl alcohol)- (PVA)- and polyamide-6,6- (PA)-based nanocomposites were prepared from dispersions by electrospinning in this study. The clays were used with PP, PVA, and PA66, but the nanoTiO_2 was used only with PVA. PVA was synthesized in the presence of both fillers and PA66 was synthesized only with clays. Spontaneous exfoliation of the clay sheets in water and formic acid was utilized with PVA and PA66. On contrast, the natural and modified clays do not spontaneously disperse in a polypropylene melt and therefore, polypropylene-based compatibilizers were added to enable the matrix to penetrate between the clay sheets. If the challenge is to exfoliate clay, the difficulty with nanoTiO_2 lay in inhibiting the formation of agglomerates. The nanoTiO_2 particles were coated with hydrophilic coatings in order to inhibit formation of agglomerates and increase miscibility with the PVA and water.

The publications I, II, and IV and some unpublished data introduces and discusses the studies of the PP/nanocomposites. The study of preparing polymer nanocomposites began by rendering the natural clay more organic in nature and preparing the well-controlled functionalized-polypropylene, PP-*co*-OH compatibilizer. The goal was to deepen the understanding of the structure-property relationship between the nanostructure and properties of the polymer nanocomposites. Later commercial grades of organomodified clays and polymer compatibilizers were utilized. A non-polar PP-based wax, which is actually a swelling agent for clay, was also evaluates as a compatibilizer. At the beginning of the study, the PP-grade was an injection molding grade and at the end an extrusion grade was used for the film applications.

Publications III and V are about producing a coating by electrospinning of the PVA and PA66-based dispersions. The first steps were to create polymerization conditions for PVA and PA66 in the presence of a suitable clay type and the last steps involved electrospinning PVA/nanoTiO_2 dispersions. The publications III and V show the importance of the preparation phase and they demonstrate the power of chemical modification of the polymer and the filler particle surfaces.

3.1 Nanostructure of PP-based clay composites

The crystalline structure of the PP-matrix has an effect on the mechanical properties of the nanocomposites. Besides molecular weight, crystallinity, and spherulite size, the α and β crystalline structures of PP influence its mechanical properties.[104,105] The mechanical performance of the β crystalline PP structure has been found to be better than that of the of α crystalline PP structure.[106,107] Particles can act as nucleating agents and the nucleating efficiency is dependent on the particle size. Nanosized fillers improve the nucleating efficiency through influencing the crystalline structure of the polymer. Spherulite size decreases and crystallinity rate increases when nanosized fillers replace micro-sized fillers.[108-110]

The influence of the presence of the nanoclay in the PP-matrix was studied for the reasons mentioned above. The concentration of PP-matrix varied from 70-wt% to 94-wt% and the concentrations of the compatibilizers and the organoclay varied accordingly. The isotactic extrusion grade PP was completely in the α-form and it was not affected by the addition of the organoclay by melt blending. The relative proportion of nanostructure in the clay varied in the nanocomposites, but it did not change the crystalline structure of the PP-matrix. The structure was studied by X-ray scattering, but the data is unpublished.

The cations of natural clay, montmorillonite, were exchange to N-methylundecenylamine (organoclay11) and octadecylamine (organoclay18) in aqueous solution, which is described in detail in publication I. The cation exchange widened the distance between the layers from the original distance, as shown in Table 4. The spacing was wider with the longer alkyl chain amine than with the shorter alkyl chain amine.

The highly polar polypropylene-grafted maleinic anhydride compatibilizer (PP-*g*-MA) and the significantly less polar hydroxyl-functionalized polypropylene compatibilizer (PP-*co*-OH) were intended to penetrate into the galleries of the N-methylundecenylamine- and the octadecylamine-modified clays and thus enable the polypropylene matrix to penetrate the clay layers too. The desired fully-exfoliated clay structure was achieved with high concentrations of the compatibilizer and clay (Table 4). The intercalated clay structure was obtained with both compatibilizers with organoclay18 with the low concentrations of compatibilizer and clay. The space between the clay sheets of the organoclay11 was not widened with low concentrations of compatibilizers and clay. It seemed that a sufficiently high concentration of the compatibilizer relative to the modified clays enables the exfoliation regardless of the space created by the alkyl amine cation. When the lower concentration of the compatibilizer relative to the clays was used,

again the spaces between the layers determined the clay structure in the polymer composite. However, the X-ray scattering techniques reveal the characteristics of the organized structure. In other words, the intercalated and original structure of the clay can be detected with this technique. The exfoliation can be detected based on the absence of signals for organized structures and therefore it cannot be observed if any organized structure is present. Moreover, the relative proportion of the different structures of the clay cannot be determined by X-ray measurements, and so the structure of the polymer composites needed to be analyzed by other means as well.

The clay structures were studied with two types of microscopes, TEM and SEM. Three types of clay structure, original, intercalated, and exfoliated, were found in the injection molded composite samples. As mentioned earlier, the exfoliated structure does not exhibit X-ray deflections.

Nanostructure was found in the clays in those samples with the PP-*co*-OH compatibilizer in the fracture surface images of the composites in the SEM and TEM images. More exfoliated and intercalated clay structure could be detected by observing the fracture surface by SEM. A rough surface at the fracture indirectly indicates that the a great relative proportion of exfoliated clay. The fracture surface was smoother in the SEM images when the concentration of the PP-*co*-OH compatibilizer was equal to the concentration of the modified clay than when it was double of the concentration the modified clay, which indicates an cohesion fracture. The result was in line with the X-ray analysis. Interpenetration of the PP-*co*-OH compatibilizer and the matrix is possible, as seen in the PP/PP-*co*-OH/modified clay, and this indicates that the PP-*co*-OH favors interactions with the outer surface of the modified clay particles, and only secondarily interacts with the inner surfaces of the clays. This means that it embeds the clay layers first and then penetrates between the layers, and the polypropylene matrix follows this behavior. The PP-*g*-MA compatibilizer seems to act in an opposite manner. It interacted with the interlayers of the clay more than the PP-*co*-OH compatibilizer and resulted in more exfoliated and intercalated structures in all composites in the SEM and TEM images than when the PP-*co*-OH compatibilizer was used.

Table 4. Characterization of polypropylene, cation exchanged layered clay (organoclay11 and organoclay18), and polypropylene/clay nanocomposites (data from I).

Materials	Composition	Interlayer distance (Å)[a]
PP	100	
Natural clay	100	9.7
Organoclay11	100	14.0
Organoclay18	100	18.8
PP/PP-*co*-OH1/organoclay11	90/5/5	14.2
PP/PP-*co*-OH1/organoclay18	90/5/5	25.7
PP/PP-*g*-MA/organoclay11	90/5/5	14.3
PP/PP-*g*-MA/organoclay18	90/5/5	33.0
PP/PP-*co*-OH3/organoclay11	70/20/10	mostly exfoliated
PP/PP-*co*-OH4/organoclay18	70/20/10	Exfoliated
PP/PP-*g*-MA/organoclay11	70/20/10	Exfoliated
PP/PP-*g*-MA/organoclay18	70/20/10	Exfoliated

The different nanostructures in the aforementioned polymer nanocomposites inspired further investigations of adhesion and compatibility. The results are in publications II and IV, and some of the data are unpublished. The clay filler was changed to commercial organically modified clay, abbreviated organoclay. Additional shear forces were created by adding filler to the melt blending. This is a fire retardant agent, aluminum tetrahydroxide (ATH), with or without a coating layer on the surface. It is a hard-edged particle. In the melt blending the hard-edged particles increase stresses[1] and grinds the clay particles, which, in turn, assists the exfoliation of the clay sheets. Compatibility of the ATH particles and the PP-matrix was intended to be improved with a stearic acid (SA) coating and/or the PP-*co*-OH or PP-*g*-MA compatibilizers in our studies. The ATH particles increased the relative proportion of the exfoliated clay structure as described in more detail in publications II and IV.

The adhesion between the components was studied by adding one ingredient at a time. The nanostructure was, again, studied by examining the fracture surfaces of the composites. The emerging ATH particles were an indication that the compatibilizer favored interactions with the organoclay instead of the ATH particles. The SA-coating treatment of ATH particles reduced the adhesion with the PP-*g*-MA compatibilizer but it increased the adhesion with PP-*co*-OH. The

influence of the stearic acid coating in the adhesion will be discussed more in the chapter on mechanical properties.

When the ATH particles and the organoclay were present in the composites, the two compatibilizers reacted in different ways, as expected based on the earlier study with the same compatibilizers. Here again, the PP-*g*-MA preferred interactions with interlayers of the organoclay, producing an exfoliated and intercalated structure. The PP-*co*-OH favors interactions with the ATH particles, and it embedded the ATH particles more completely than the PP-*g*-MA, and the structure of the organoclay was less exfoliated.

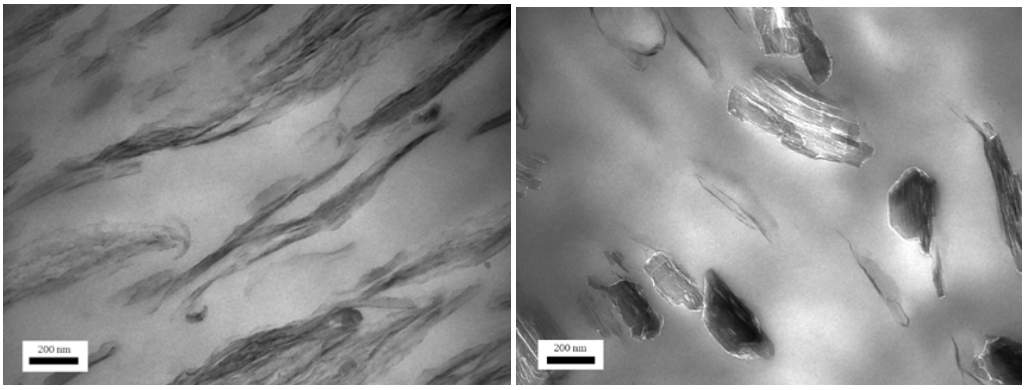

Figure 2. Transmission electron microscopy images of composite: PP/organoclay/PP-*g*-MA (left) and PP/ATH/organoclay/PP-*g*-MAH (right) (reproduced from II).

The compatibilizers discussed above are polar and a different approached to exfoliating organoclay was studied. Polypropylene-based paraffin wax compatibilizer, abbreviated PPwax, was used instead of the laboratory scale PP-*co*-OH compatibilizer (unpublished). It was melt blended in a continuous co-rotating extruder with an extrusion grade polypropylene matrix and the organoclay. The PPwax was melt blended with the other components instead of allowing the clay to absorb wax, because the aforementioned compatibilizers were melt blended in publications I, II, and IV. However, the earlier studies cannot be compared with this study, because the PP-grade and the melt blending extruder were different. Previously, the composites were prepared with an injection molding grade PP and in a 15 min batch midi-extruder, and here they were prepared with an extrusion grade PP and a continuous scaled-up extruder.

The structure of the clay in the polymer matrix was characterized with X-ray measurements as presented in Figure 3. The relative proportion of nanostructure was maximal when the concentration of organoclay and PP-*g*-MA compatibilizer was 5 wt-%, or less than in the PP/organoclay composites. This result is opposite to those from the earlier studies, where the higher

concentration of the compatibilizer and the modified clay increased the relative ratio of nanostructure. The maximum relative proportion of exfoliation was obtained at 5 wt-% or more, when PPwax compatibilizer was used in the PP/organoclay composites, but some microsized particles were observed. Microsize clay particles were not observed when the PP-*g*-MA compatibilizer was used. In other words, the interaction between the PP-g-MA compatibilizer and the organoclay was stronger than the interaction between the PPwax compatibilizer and the organoclay.

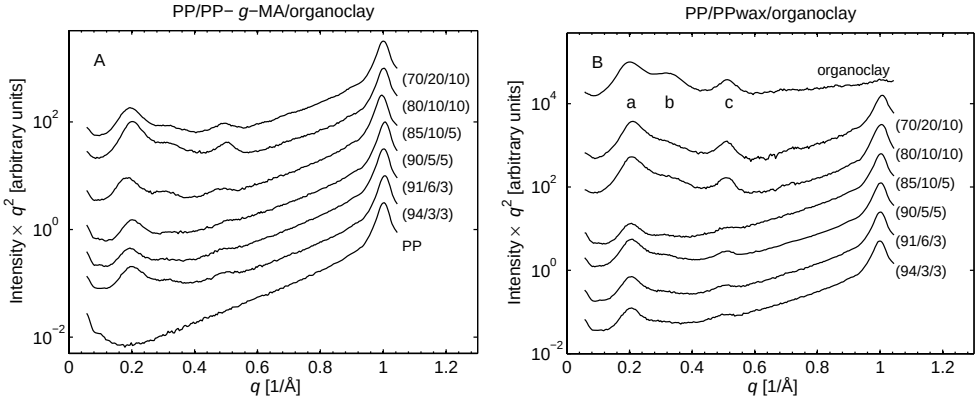

Figure 3. A) Lorentz-corrected SAXS intensities on a logarithmic scale from pure PP and PP/PP-*g*-MA/organoclay composites. B) SAXS curves of PP/PPwax/organoclay and pure organoclay. The reflections of organoclay are marked with the letters a (d = 31.4 ± 0.4 Å), b (d = 23 ± 1 Å) and c (d = 12.6 ± 0.1 Å) (unpublished data).

3.2 Melt viscosities of PP-based nanoclay composites

Melt viscosity indirectly indicates the adhesion between the components, and is influenced by the structure of the filler particles and the polymer. The packing fraction of the filler and the molecular weight and polarity of the compatibilizer[111,112] influence melt viscosity. The molar weight of the PP-*g*-MA compatibilizer was similar to that of the PP-matrix and the molecular weight of the PP-*co*-OH compatibilizer was at least one order of magniture lower than the PP-matrix. The low molecular weight is intended to decrease the melt viscosity. The rheological characterization is partly presented in publication II and the rest is presented in the following discussion.

The addition of organoclay11 to the PP-matrix increased melt viscosity, as expected, due to an increase in shear stress caused by the clay microsize particles. The melt viscosities of the PP-based clay nanocomposites were lower than those of the PP-matrix when the concentration of

the compatibilizer and the filler were at 5-wt%. Moreover, the PP-*g*-MA compatibilizer decreased the melt viscosity more than the PP-*co*-OH compatibilizer. The dominant nanostructure type was intercalated rather than exfoliated and, further, a wider intercalated structure was achieved with the PP-*g*-MA compatibilizer than with the PP-*co*-OH compatibilizer. The concentrations of the compatibilizers seem to be low enough not to influence dramatically the melt viscosity. The PP/PP-*co*-OH/clay (90/5/5) melt viscosity is at low frequencies is higher than that of the PP and this is most probably due to the high concentration of the microsized clay particles.

The higher concentrations of the compatibilizer (20-wt%) and clay (10-wt%) increased the relative proportion of exfoliated structure of the clay and, again, the melt viscosities were lower than those of the PP-matrix with the exception of the PP/PP-*g*-MA/organoclay11 (70/20/10). In turn, the lowest melt viscosities were measured with the composites including the PP-*co*-OH compatibilizer. Further, the organoclay11, which had narrower spacing between the sheets than the organoclay18, decreased the melt viscosity more than the organoclay18 regardless of the compatibilizer. The concentration of the clay, in other words, the packing fraction and molecular weight of the compatibilizer were at a level where they influenced the melt viscosity more than the effect of nanostructure did. In other words, the clay particles increase the melt viscosity of the PP-matrix as shown in Figure 4, but nanostructure up to a certain point, nanostructure decreases the melt viscosity. The more extensive the exfoliation and the higher the concentration of clay in any structure and the more the clay surface attracts the compatibilizer, the more melt viscosity is increased.[113] As the relative surface of the clay exposed to the compatibilizer increased, the interaction between them increased resulting in an increase in melt viscosity. In addition, the higher polarity of the PP-*g*-MA relative to PP-*co*-OH causes PP-*g*-MA to interact more strongly with the clay sheet surface, which, in turn, results in higher melt viscosity.

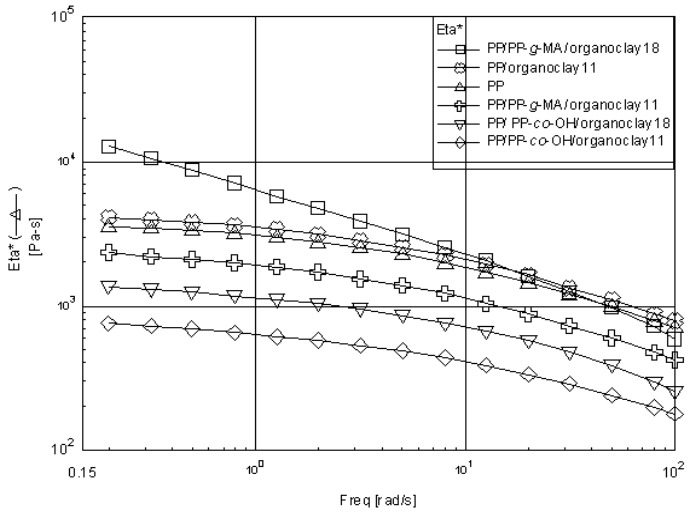

Figure 4. The melt viscosities measured at 210°C of composites composed of 10 wt% of organoclay(11 and 18) with or without compatibilizer at 20 wt-%, and neat PP (II).

The melt viscosity was influenced by the structure and the concentration of the nanoclay and the concentration and the molecular weight of the compatibilizer. If the molecular weight of the compatibilizer is similar to the molecular weight of the matrix, the molecular weight becomes trivial in melt viscosity. When the molecular weights of the polymers in the blend differs, the melt viscosity behavior of the polymer blend adopts melt behavior of the polymers in the blend.

The PPwax had a significantly lower molecular weight than the PP-matrix. When PPwax was used as the compatibilizer in the PP/clay composites, the shear stresses increased as the concentration of the organoclay and compatibilizer decreased in the composites as shown in Figure 5. The PPwax was not able to enhance the formation of the clay nanostructure and it caused a decrease in melt viscosity. The increase in concentrations of clay and PPwax did not change the shear stress. The PP-*g*-MA compatibilizer in the composites increases the nanostructure of the clay, and causes a similar increase in the melt viscosity. Again, it is to be noted that the clay structure and molecular weight of the compatibilizers and thus polarity differed in these composites.

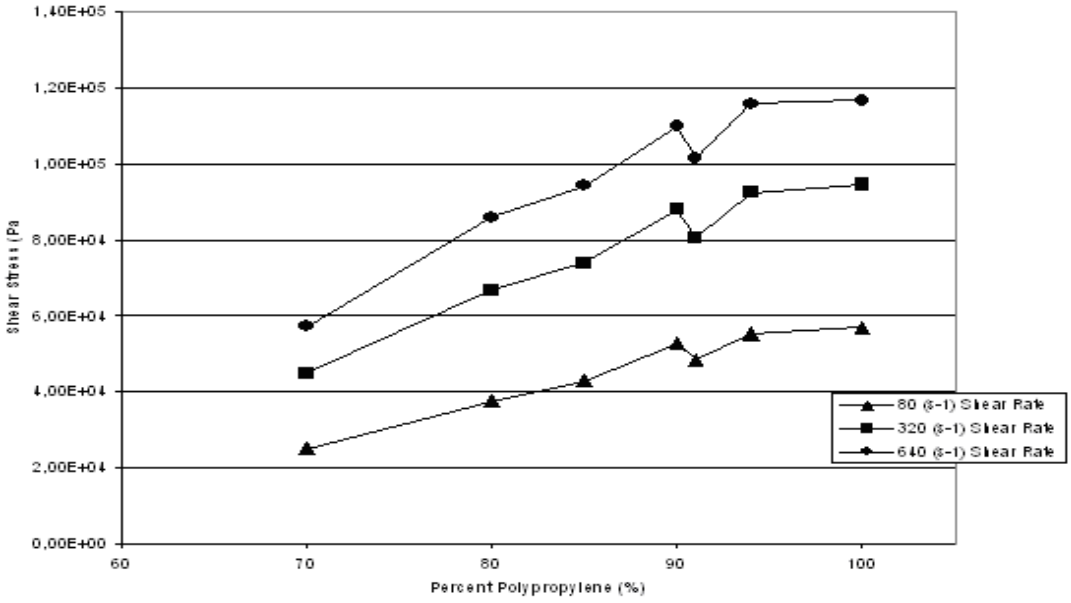

Figure 5. Mass fraction of polypropylene that affects the shear stress for different shear rates of the PP/compatibilizer/nanoclay composites, when PPwax is used as the compatibilizer (Unpublished data).

3.3 Mechanical properties of PP-based clay nanocomposites

Stiffness-toughness properties were studied with a spectrum of PP-based nanocomposites. Table 4 is an overview of the results presented in publication II and the unpublished data. The extrusion grade PP had a higher tensile modulus and lower elongation of break to begin with than the injection molded grade PP.

Addition of the organoclay to the neat injection molding grade PP with or without a compatibilizer increased the tensile modulus dramatically, while toughness decreased. The compositions were very fragile. The compatibilizer was partly substituted for by the PP-matrix and thus the amount of fillers was kept at 30-wt% and the amount of polymer was correspondingly kept at 70-wt%. The compatibilizers enabled the formation of the clay nanostructure in the PP-based composites, but they did not have a dramatic influence on the mechanical properties of the PP/clay composites, which was not expected. The reason could be that the concentration of the compatibilizer was too low. It has been earlier noted that a sufficient amount of compatibilizer is needed to enhance the compatibility between the matrix and the interlayers of the modified clays. However, the concentration of the clay was kept at this high level in order to verify the in influence of the additional shear forces on the proportion of exfoliated clay.

Addition of ATH particles to the PP-matrix increased the tensile modulus and decreased the toughness, but less than addition of the organoclay. The addition of PP-*g*-MA to the

PP/ATH composite decreased the tensile modulus, as shown in Figure 6. Addition of the organoclay and the PP-*g*-MA compatibilizer to the PP/ATH composite (with or without stearic acid treatment) decreased the tensile modulus and increased the elongation at break moderately. The addition of the organoclay and the PP-*co*-OH compatibilizer to the PP/ATH composite decreased the tensile modulus (Figure 6) and increased the elongation at break.

The addition of the organoclay and the compatibilizer lowered the toughness and stiffness of the PP/ATH composites, except for the PP/ATH(SA)/organoclay/PP-*co*-OH composite. Here the toughness increased but the stiffness decreased by an order of a magnitude below that of the aforementioned composites.

The compatibilizers in the PP/ATH/organoclay composites reacted differently to the stearic acid treatment of the ATH particles. The stearic acid coating of the ATH particles did slightly strengthen the interfacial interaction of PP-*g*-MA compatibilizer with the organoclay. The SA coating increased the interaction between the stearic acid coating and the PP-*co*-OH compatilizer and less exfoliated clay structure was formed, and therefore the toughness increased as for the PP/organoclay composite. It seems that the concentration of the PP-*co*-OH compatibilizer was not sufficient to interact with the organoclay is such a way as to enhance formation of nanostructure in the clay.

Addition of the organoclay and a compatibilizer to neat extrusion grade PP moderately increased the tensile modulus, while toughness did not decrease in all the composites. In fact, when low concentrations (Table 5) of the organoclay and compatibilizers were used, both stiffness and toughness increased. The high concentration of the organoclay and the compatibilizers increased stiffness and decreased toughness. The explanation could be the exfoliation of the clay which was found to be relative high proportion with high concentrations of the PPwax and with low concentrations the PP-*g*-MA compatibilizer. Surprisingly, the total concentration of the compatibilizer and organoclay had a major influence on the stiffness-toughness, while the degree of exfoliation had less influence.

When the organoclay was added to the PP-matrix, the increase in modulus was less significant for the extrusion grade than for the injection molding grade PP. On the other hand, the decrease in elongation at break was less for the extrusion grade than for the injection molding grade. Exfoliation was observed as an increase in tensile modulus and this is probably due to the increase in the aspect ratio of the clay. Moreover, the relative surface area of the organoclay increases as the concentration of the organoclay increases regardless of the structure of the added organoclay.

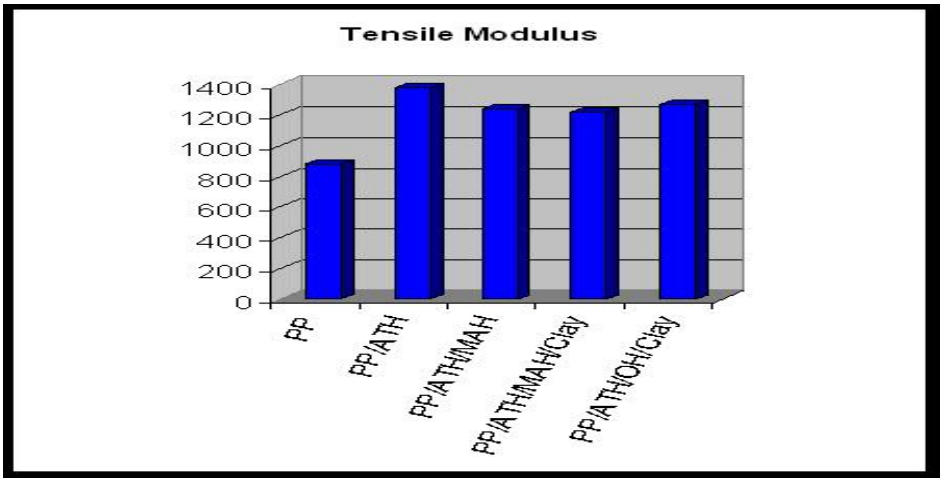

Figure 6. Tensile modulus of polypropylene, PP/ATH, PP/ATH/PP-*g*-MAH, PP/ATH/PP-*g*-MAH/organoclay, and PP/ATH/PP-*co*-OH/organoclay composites.

Table 5. Tensile modulus (E), tensile strength (σ), and elongation at break (ε_b) for injection molding and extrusion grade PP and nanocomposites (reproduced from II and IV and unpublished data).

Material	Ratio	*E* (MPa)	S.D.	σ (MPa)	S.D.	ε_b (%)	S.D.
PP injection molding grade	100	876	10.3	39.6	0.2	1186.8	24.2
+organoclay	70/30	1600	46.1	34.0	1.1	5.3	0.5
+organoclay/PP-g-MA	60/30/10	1725	33.2	33.9	0.6	5.7	0.4
+organoclay/PP-co-OH	60/30/10	1338	13.4	34.1	0.4	7.8	0.4
+ATH	70/30	1379	42.9	31.1	11	114.8	44.1
+ATH/organoclay/PP-g-MA	60/25/5/10	1216	28.3	33.1	0.3	48.7	6.0
+ATH(SA)/organoclay/PP-g-MA	60/25/5/10	1243	29.6	32.6	0.5	53.8	9.6
+ATH/organoclay/PP- co-OH	60/25/5/10	1272	35.8	37.4	0.2	12.9	1.7
+ATH(SA)/organoclay/PP-co-OH	60/25/5/10	1460	25.1	35.2	0.7	9.0	0.7
PP extrusion grade	100	1270	6	34.6	0.2	317	15
+PP-*g*-MA/organoclay	90/5/5	1370	24	42.8	0.2	43	7
+PP-*g*-MA/organoclay	80/10/10	1480	35	33.4	0.9	8	3
+PPwax/organoclay	90/5/5	1490	36	34.9	0.8	11	3
+PPwax/organoclay	80/10/10	1540	62	31.4	0.6	4	0

3.4 Melting and crystallization behavior of PP-based clay nanocomposites

The melting and crystallization behavior of the PP/ATH/organoclay nanocomposites can be used to study the relative proportion of clay exfoliation and the interfacial adhesion between the components. Particles can act as nucleating agents and the nucleating efficiency is dependent on the particle size. Nanosized fillers improve the nucleating efficiency by influencing the crystalline structure of the polymer. Spherulite size decreases and crystallinity rate increases when nanosized fillers replace micro-sized fillers.[108,109,110] Good nucleating agents increase the temperature where the PP begins to crystalline.

The addition of ATH with or without stearic acid (SA) coating and/or organoclay increased the melting temperatures of the PP. The melting temperatures of the PP/ATH-based composites were all similar. The significant crystallization temperature rise was due to the ATH particles, not the organoclay. A clear difference in the crystallization behavior was observed and it depended on the PP-based (nano)composite, as shown in Figure 7. The crystallization temperatures varied between the crystallization temperatures of PP and PP/ATH/PP-*g*-MA.

The crystalline structure of the PP-matrix influences the thermal properties: PP with an α crystalline structure PP melts at lower temperature than PP with a β crystalline structure. However, the PP structure was not influenced by the addition of the fillers separately or together, according to the X-ray measurements, and thus the changes in the melting and crystallization temperatures are due to the fillers.

The addition of ATH particles increased the PP-matrix crystallization temperature significantly, unlike addition of organoclay. The ATH particle seems (with or without SA coating) to act as an excellent nucleating agent and the organoclay particles less so. The PP-*g*-MA compatibilizer increased the crystallization temperature above that of PP/ATH and, PP/ATH(SA). The high crystallization temperature of the PP/organoclay/PP-*co*-OH is most probably due to the low molecular weight of PP-*co*-OH, not the organoclay. The molecular weight of PP-*co*-OH is lower than that of the PP-matrix and PP-*g*-MA compatibilizer.

The stearic acid coating of the ATH particles interfered with the interaction between the PP-*g*-MA compatibilizer and the ATH(SA) particles and the result was an decrease in the crystallization temperature even in the composites where ATH was partly substituted for by the organoclay. The partial substitution of ATH particles with organoclay decreased the crystallization

temperature for the PP/ATH-based composites. This was expected due to the non-nucleating effect of the organoclay.

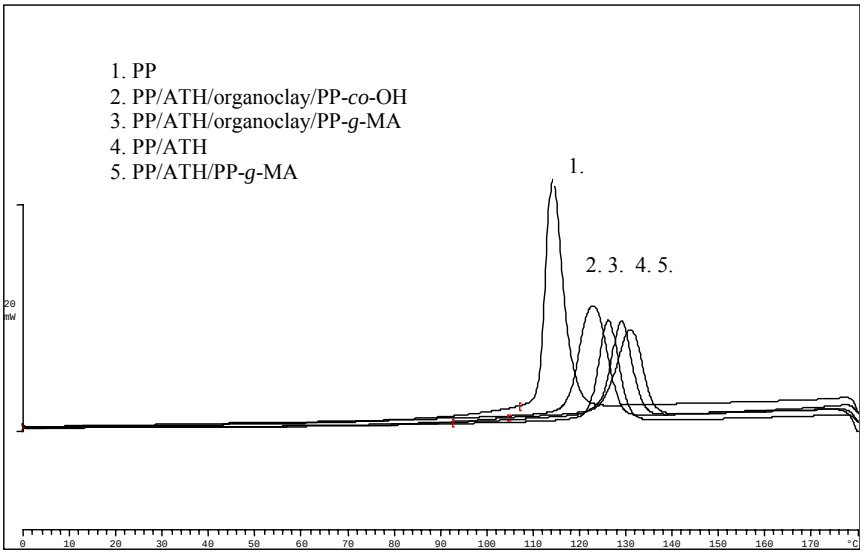

Figure 7. Cooling thermograms of PP, PP/ATH composite, PP/ATH with PP-*g*-MA compatibilizer, and PP/ATH/organoclay with compatibilizers (II).

3.5 Flame retardant properties of PP/ATH nanocomposites

Absorption and diffusion properties of nanoclay composites are based on two phenomena: sheets absorb and/or bind volatile molecules and long diffusion paths create the so-called the labyrinth effect.[8, 12, 14] Flame retardant properties of polymer/nanoclay composites are based on the same mechanisms as for those for absorption and diffusion. In addition, char formation of layered clay during combustion acts as a thermal insulator and a barrier against heat and mass transport. From this point of view, the exfoliated clay structure is more efficient than the intercalated clay structure or micro-sized particles. ATH absorbs heat and releases water. The fire-retardant properties of the PP/ATH composites and PP/ATH/organoclay composites were studied and presented in publication II.

Peak heat release rate (HRR) and total heat released were, naturally, high for the neat PP and they were reduced in the composites containing ATH and/or organoclay, as shown in Figure 8. Unexpectedly, the addition of organoclay to PP reduced the HRR more than the addition of ATH. When both of them were added, the HRR values were between the values detained when the fillers were used separately. Time to ignition was delayed when ATH was added to the PP-matrix. The

rest of the composites ignited within a narrow time frame, except the PP/ATH/organoclay/PP-*g*-M, which ignited faster than PP and the other composites.

In other words, synergy was not created by combining these two fillers. The concentration of ATH used was not sufficient to inhibit fire. The same concentration of organoclay, on the contrary, inhibited the fire more. This could be due to the difference in the flame retardant method. The 30-wt% of organoclay was able to create a protective char layer, but the ATH was not able to release enough water to extinguish the fire. The partial substitution of ATH for organoclay reduces the flame retardant properties. The protective char layer was not formed due to the thin exfoliated clay sheets and the low concentration of the clay.

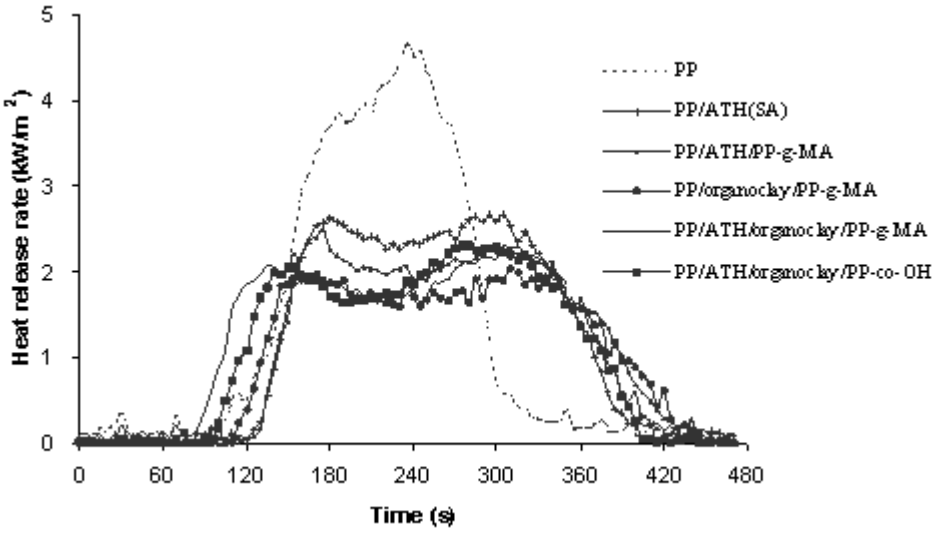

Figure 8. Comparison of the heat release rate (HRR) plots of neat PP and PP/ATH/organoclay composites of different compositions (II).

3.6 Diffusion properties of PP-based clay nanocomposites

Water and oxygen diffusion properties of the PP/organoclay composite membranes were measured, and the results were published in "**Nordic Rheology Conference in 2006**" by Ristolainen *et. al*. The PP was extrusion grade, which is intended to be used in film applications. The compatibilizers were PP-*g*-MA and PPwax.

Water vapor absorption was lower when the PP-*g*-MA was used as a compatibilizer instead of the PPwax, which might be expected because fever clay agglomerates were present when the PP-*g*-MA compatibilizer was used instead of PPwax. The absorption of water vapor was greater

in nanocomposites than in the neat PP, which might be expected due to the filler loading creating voids between the filler and the matrix and the possible hydrogen bonding between water and hydroxyl-groups on the clay surface[114,115]. It was seen that the compatibilizers and the degree of exfoliated organoclay determined the absorption rate. The highest degree of exfoliated organoclay was observed with low loading of the organoclay in the PP/PP-*g*-MA/organoclay nanocomposites and with high loading of the organoclay in the PP/PPwax/organoclay nanocomposites. It is reasonable that the permeated water depended on the structure of the organoclay. The intercalated structure is able to absorb water between the layers, which results in higher quantities of absorbed water than in the composites with an exfoliated structure. This was observed in the measured samples. Water vapor permeating through the PP/PP-*g*-MA/organoclay films increased as the concentration of the organoclay *i.e.* relatively more intercalated structure, was increased. The opposite was observed with PP/PPwax/organoclay films. As the concentration of the organoclay increased (relatively more exfoliated structure) the permeation decreased.

It is of interest to know the transport rate of oxygen in packaging applications and therefore the oxygen barrier properties of PP/organoclay membranes were studied. The organoclay was mostly in the exfoliated form in the PP/organoclay composites when low concentrations of the organoclay were used and therefore only these samples were subjected to the measurements. The electric current was recorded as a function of time, and the diffusion coefficient and solubility wwere calculated. This is described in more detail in the publication by Lehtinen *et al.* [116]

A reduced oxygen diffusion rate was achieved with the PP/PPwax/organoclay composites, while the oxygen diffusion rate increased moderately with the PP/PP-*g*-MA/organoclay composites, as shown in Table 4. Solubility and permeability values of the PP/organoclay composites approached those in PP as the organoclay and compatibilizer concentrations increased. This is due to the increase in the volume fraction of the hydrophilic organoclay. Water from the air is trapped between the organoclay layers, inducing a higher oxygen solubility and permeability. Single sheets of exfoliated structure are not able to hold water like the intercalated sheets do.

Table 6 Oxygen diffusion coefficient (D), solubility (c), and permeability (P) of selected PP/organoclay composites

Membrane	Ratio	D (cm^2/s) $\times 10^{-7}$	c (mol/ cm^3) $\times 10^{-6}$	P (g/ ms) $\times 10^{-9}$
PP	100	4.2	3.7	5.0
+PP-*g*-MA/organoclay	91/6/3	4.9	2.1	3.3
+PP-*g*-MA/organoclay	90/5/5	4.8	2.1	3.2
+PP-*g*-MA/organoclay	85/10/5	4.3	4.1	5.6
+PPwax/organoclay	91/6/3	2.3	5.1	3.8
+PPwax/organoclay	90/5/5	3.8	6.5	7.9
+PPwax/organoclay	85/10/5	4.1	8.9	12.0

3.7 PVA- and PA66 –based nanoclay dispersions

Several poly(vinyl alcohol) (PVA) and polyamide-66 (PA66) nanoclay dispersions were prepared and the interaction between the components was analyzed indirectly by measuring the dispersion viscosities. The miscibility of the clay set the limits on the type of clay to be used in the dispersions. Natural clay delaminates in water and it is not miscible with organic solvents; and the situation is reversed for the organomodified clay. The dispersions are summarized in Table 7. The final goal was to electrospin a fine coating network with evenly distributed nanoclay along the polymer fibers and the dispersion viscosity could be one tool to tailor the network. The dispersions were prepared by two methods as described in the Experimental section and in publication III: the PVA and PA66 were synthesized in the presence of clay, or the components were mixed in suitable solvents.

The functional groups of PVA influence the interactions between the polymer-water, polymer-polymer, and polymer chain with itself, which influences the solution/dispersion viscosity. The PVA chain possesses functional groups like hydroxyl groups along the chains, and other functional groups can be introduced to it, such as carboxyl- and silanol-groups. The dispersion viscosities decreased when the carboxyl- or the silanol-groups were added to the PVA, except for the ones which formed a gel. The clay was added in these studies simultaneously, before, or after the polymer and in all dispersions the dispersion viscosity was highest without the carboxyl- or silanol-groups. In other words, the dispersion viscosities were greatly influenced by the functional groups of the polymer. However, the preparation conditions influenced the dispersion viscosity levels.

The PVA/clay dispersion had a higher dispersion viscosity than the carboxyl-functional PVA when the pH was changed from alkali to acidic. (The silanol-functional PVA/clay dispersion formed a gel.) The difference between the highest and the lowest viscosity was greater in alkaline conditions than in acidic conditions. The PVA-water interaction and the carboxyl-PVA-water interaction were different from each other. The decreased viscosity of the nanoclay-filled unmodified PVA disperison and increased viscosity of nanoclay-filled functionalized PVA dispersion. More over, they completely different from than of the silanol-functional PVA/clay dispersion. However, the molecular weight could have an influence to the dispersion viscosities, but the respective polymer can be compared with each other even if not directly with the PVA with other functionalities.

The feeding order of the components changed the dispersion viscosity as well. Again, the PVA-based dispersions had higher viscosities than the carboxyl-functional PVA-based dispersions. The dispersion viscosity levels increased by tenfold when the clay was allowed to delaminate in water, not dissolving the polymer before adding clay (from A to B in Table 7). The high dispersion viscosities of the B-series are due to the complete exfoliation of the clay. The exfoliated clay has the highest specific area the clay can achieve, which, in turn, enables the maximum interaction between the polymer and the clay surface.

The poly(vinyl alcohol)/nanoclay dispersion was also prepared by emulsion polymerization from vinyl acetate monomer in water. The emulsion polymerization of poly(vinyl acetate), (PVAc) which is the prepolymer for the poly(vinyl alcohol), could be carried out in the presence of the natural clay. The natural clay delaminates completely in water and, thus the growing polymer chain would evenly embed the single clay sheets. The alcoholysis of PVAc does not effect the clay distribution in the dispersion, because the reaction changes the functionality of the carboxyl groups of the PVAc. The dispersion viscosity cannot be compared to the above mentioned dispersions, because the degree of hydrolysis, the molecular weight, and the structures of the PVAs used are not know and thus not comparable. Dispersion viscosity of PVA synthesized in the presence of natural clay was 760 cP.

Table 7. Measured viscosities of the pre-spun dispersion of neat PVA (n-PVA), PVA with carboxyl groups (a-PVA) and silanol groups (f-PVA) with clay, when the pH of the solution and the feeding order of the components were changed, and PA with organoclay and clay with changing feeding order.

	Viscosity (cP) in the pH[a] study		Viscosity (cP) in the Feeding order[b] study	
Polymer in the mixed dispersion	Alkaline (9-10)	Acid (1-2)	A series	B series
n-PVA	435	380	860	4600
f-PVA	275	Gel	850	Gel
a-PVA	205	300	450	3340
PA66[c]	-	-	115	115
PA66	-	-	130	130

Synthesized polymer in the presence of filler	Viscosity, cP
s-PVA[C]	760
s-PA66	370

a ratio of PVA/clay 4:1
b ratio of PVA/clay 10:1
c clay was organoclay

Polyamide-6,6 (PA66) was mixed with natural clay and commercial organomodified clay. The feeding order of the components was, here again, varied: PA66 was dissolved in formamide before addition of (organo)clay or (organo)clay was added to formamide before dissolving PA66 in dispersions. However, the feeding order of the components had no effect on the dispersion viscosities, which were 115 cP and 130 cP. The moderate difference in the dispersion viscosities was due to the clay used, because only the clay type changed in these studies. The natural clay is more compatible with the polyamide/formamide solution than the organoclay, because of its polar nature. The better miscibility, in other words better compatibility, results in higher dispersion viscosity. The higher dispersion viscosity of the PA66/clay than of the PA66/organoclay is due to the stronger interaction with the polymer and the delaminated clay sheets.

The step polymerization of PA66[46] was successful when natural clay was in the water phase, but not when the organomodified clay was in the organic phase. The dispersion viscosity of the PA66/nanoclay was 370 cP. It was not within the scope of this study to reason why the organomodified clay inhibited the step polymerization. The organomodified clay might have

interfered with the polymerization by hindering the monomer contacts or trapping the leaving groups.

3.8 Electrospun fiber network of PVA and PA66 nanoclay composites

The viscosity of the dispersions was one of the main factors influencing fiber formation in electrospinning. It was relatively easy to change the viscosities of the PVA-based dispersions by changing the concentration of the clay, the dispersion pH, and the feeding order of the components. The PA66-based dispersions, on the other hand, were influenced less than the PVA-based dispersions by changes in the hydrophobicity of the clay and the feeding order of the components as seen in Table 7. Every system has a fiber-forming viscosity, and above it continuous fibers on the substrate are formed instead of stand-alone droplets. The electrospun fibers and droplets contained clay particles.

The PVA-based dispersion viscosities in the feeding order study were higher than those found in the pH-study dispersions. The increase in the polymer to the clay ratio in the dispersions increased the PVA dispersion viscosities, which in turn changed the coating pattern from a continuous circular area to distinct spots on the substrate. The electrospinning process parameters were adjusted for each of the dispersions separately to enhance fiber formation, because the aim was to achieve smooth fibers.

The change in the pH in PVA-based dispersions partially affected the fiber diameter, the fiber network structure, and the size of clay particles along the fibers, and the differences cannot be completely explained by the changed dispersion viscosities. The clay particle size was smaller under alkaline conditions than under acidic conditions, regardless of the PVA type used. This indicates that under alkaline conditions a more delaminated clay structure of clay was achieved and it could be due to the favorable interaction between the polymer and clay interlayers, because the polymers were able to intercalate between the clay layers under normal pH conditions. The fiber diameters and networks were similar for the PVA- and carboxyl-functional PVA-based dispersions regardless of the pH, and the silanol-functional PVA-based dispersions differed in producing narrower and separate fibers. The former dispersions formed continuous fiber networks and the latter formed isolated fibers, not networks.

The feeding order of the PVAs and clay greatly influenced the dispersion viscosity, as mentioned earlier (Table 7). However, the electrospun fiber networks formed were similar. It seems that the dispersion viscosities were above the fiber-forming limit and thus the increase in viscosities

had only a minor influence on the fiber diameter and the network structure. However, as stated earlier, natural clay exfoliates in water. When the clay was added to water before dissolving the PVA, the clay particle diameters along the electrospun fibers were smaller than when the PVA was dissolved in water before the clay. This was observed regardless of the PVA grade. A typical fiber network structure is presented in Figure 9.

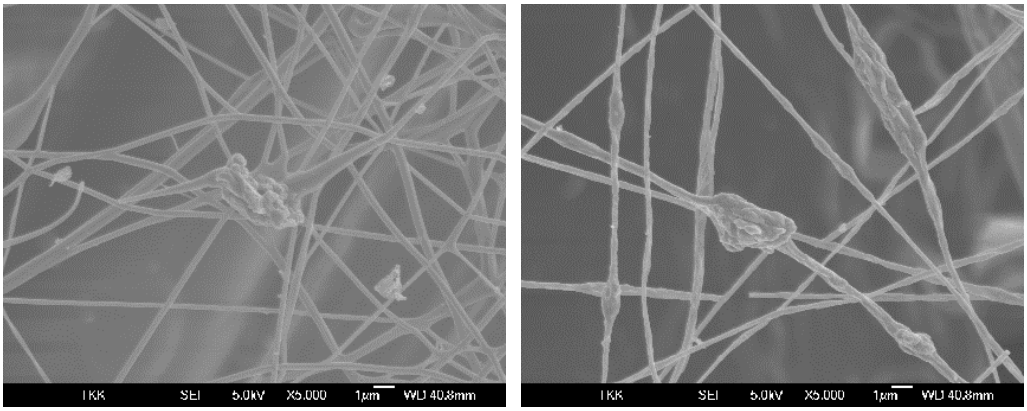

Figure 9. Typical fiber networks of PVA/clay. PVA was dissolved in water before swelling of the clay (left) and clay was allowed to swell before addition of PVA (right) (reproduced from III).

The PA66-based dispersions formed a visually smooth and continuously coated circular area with a few separate spots on the substrate, except for one where the dispersion deposited completely isolated spots. The dispersion viscosities of the PA66-based dispersion were similar between themselves and, as expected, the electrospun fiber networks appeared similar as shown in Figure 10. In addition, the size of the clay particles within the fibers was alike, with round-shaped rough-surfaced bulges. Polymer beads were also observed along the PA66-fibers. The appearance of the polymer beads differs from the appearance of the embedded (organo)clay particles.

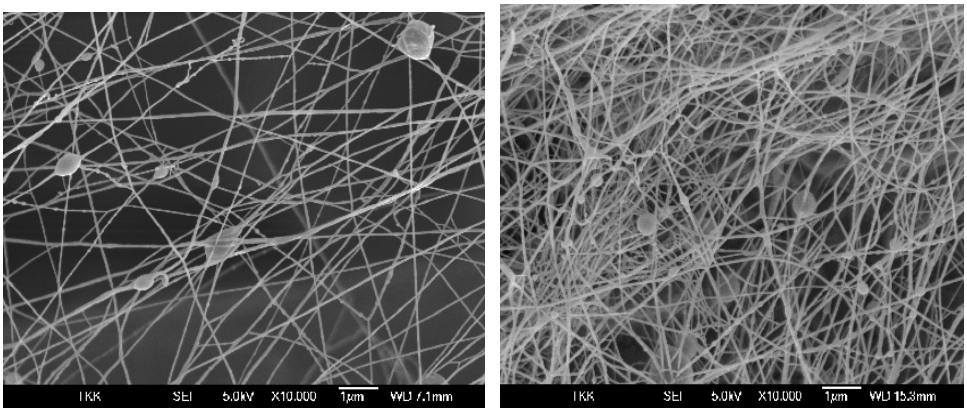

Figure 10. PA66/clay composites: A series c-PA/clay (left) and B series c-PA/organoclay (right) (reproduced from III).

The clay agglomerates along the electrospun fibers were larger than expected when the components were mixed together. The *in situ* polymerization in the presence of (organo)clay was thought to reduce the clay particle size along the electrospun fibers. The process parameters were again adjusted for the PVA/clay and PA66/clay. Again, the PA66/clay-based dispersion deposited as a continuous circular area on the substrate, like the commercial grade PA66-based dispersions, but the PVA-based dispersion produced splashes visible to the naked eye, similar to the PVA-based dispersions used in the pH study. However, the clay particles along the electrospun fibers had smaller particle diameters in both the PVA and PA66 fibers than when the components were mixed together. They were rough-surfaced roundish bulges embedded in the polymer irrespective of the size of the particle, and they were distributed within the fibers, indicating a full exfoliation before electrospinning.

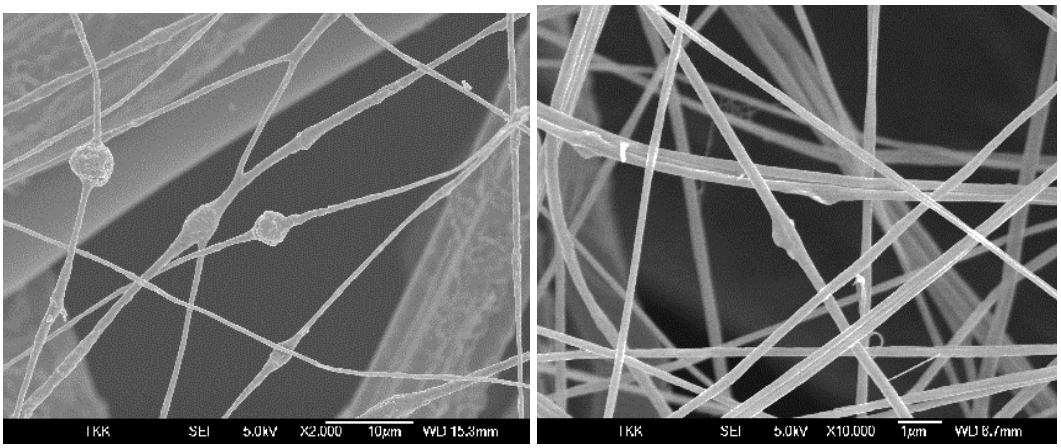

Figure 11. Electrospun fiber network of PVA- (left) and PA66- (right) based dispersions prepared by synthesis in the presence of clay (reproduced from publication III).

3.9 Coating properties of PA66/nanoclay fiber network

Contact angles and water penetration times (Table 8) were measured for the four PA66-based electrospun coated substrates introduced in the previous studies. The diameter of the coated area for the measurements needed to be more than 5 cm, and such a uniform area was not achieved with the PA66/organoclay dispersion in which the PA66 was dissolved in formic acid before the organoclay was added. The contact angle of the substrate without electrospun coating was 70° and the time for water penetration was less than 1 second. An increase in the contact angle and water penetration indicates an increase in the hydrophobicity and density of the network. As expected, the contact angles and the water penetration times increased when the substrate was coated with the commercial PA66-based electrospun coatings. The PA66 absorbs water the air.[46,53] The coated substrates were not dried before the contact angle and water penetration time measurements were carried out and it is to be assumed that the PA66 saturation level had been achieved before the tests. The organoclay-based coating resisted the water absorption longer than the clay-based coatings, which is most probably due to their respective hydrophilicity/hydrophobicity properties. The organoclay is hydrophobic and clay is hydrophilic. On the other hand, with the PA66/clay dispersion, which was prepared by synthesizing the PA66 in the presence of clay, the contact angle was smaller than and water penetration time was equal to that of the base substrate. This could be due to the more finely distributed hydrophilic clay sheets and an indication that the amount of clay was insufficient to reduce the water absorption.[53] It could be concluded also that the better the clay was exfoliated and thus dispersed along the fibers, the lower was the measured contact angle. The water penetration time followed the results for the contact angles: large contact angles go hand in hand with long water penetration times.

Table 8. Contact angles and water penetration times for PA66-based dispersions from the feeding order study (A and B order, see chapter 3.7) and the PA66 synthesized in the presence of clay (reproduced from III).

	Substrate	A PA66/clay	B PA66/clay	A PA66/organoclay	B PA66/organoclay	Synthesized PA66/clay
Contact angle (°)	70	98	72	-	100	62
Time (s)	< 1	2	2	-	4	<1

3.10 PVA/nanoTiO$_2$ dispersions

The PVA/nanoTiO$_2$ dispersions were prepared using two methods: *in situ* emulsion polymerization of vinyl acetate monomer in the presence nanosized titanium dioxide (nanoTiO$_2$) and mixing of commercial PVAs with the same nanoTiO$_2$s. The three different hydrophilic coatings of the nanosize TiO$_2$ (see Table 2) were used with the same grades of PVA used in earlier studies. The polymerization was carried out the same way as for PVA/clay, which is described in paper III and in the Experimental section. The hydrophilic coating layers on the nanoTiO$_2$ were chosen in such a manner that the filler particles were compatible with the polymerization system and the PVAs used in aqueous solution.

The addition of the nanoTiO$_2$s did not inhibit the emulsion polymerizations of acetate monomer in water. The fillers had hydrophilic coatings to ensure miscibilities in water-based reaction media during the polymerizations, but the miscibility's of the nanoTiO$_2$ particles differed: the nanoTiO$_2$ (al) was miscible, nanoTiO$_2$ (oh) was immiscible, and nanoTiO$_2$ (gl) was poorly miscible. The crystal size of the PVAc/nanoTiO$_2$ (al) was the smallest of the series and it was miscible during the polymerization. The immiscible nanoTiO$_2$ (oh), which had a larger crystal size and smaller specific surface area than the two other nanoTiO$_2$s, phase separated during the polymerization.

The PVAc with nanoTiO$_2$ (oh) had a lower molecular weight but wider molecular weight distribution than of PVAc with nanoTiO$_2$ (gl) and in addition the dispersion viscosity of the PVA/nanoTiO$_2$ (gl) was higher than that of the PVA/ nanoTiO$_2$ (oh). But the molecular weight and distribution of the PVAc with nanoTiO$_2$ (al) were between those of the aforementioned dispersions although its dispersion viscosity was clearly lower than that of the first mentioned dispersions. The nanoTiO$_2$ particles during the polymerization could have been acting as nucleating agents. It seems that even poorly miscible particles acted as nucleating agents and as the miscibility improved, the polymers were more uniform due to the large number of initiation points. However, the different behaviors miscibility of the nanoTiO$_2$ particles does not explain why the molecular weights (M_w) and the molecular weight distributions (MWD) of the PVAcs varied. In addition, the dispersion viscosities of the PVA/nanoTiO$_2$s varied even more than expected based on the M_w, M_n, and MWD.

The same three nanoTiO$_2$ particles were mixed with the unmodified PVA and with the two modified PVAs which have been used throughout the research. The dispersion viscosities varied moderately. The viscosities of the PVA grades are similar according to the manufacturer and therefore the polymer matrix itself should not influence the variation in the dispersion viscosities,

which should be a result of interactions between the polymer and the nanoTiO_2 filler. However, once again the miscibility of the nanoTiO_2 grades does not, after all, explain the differences in the dispersion viscosities. The miscibility of the alumina-coated TiO_2 was better than the miscibilities with of the two other coated nanoTiO_2s, which could explain the low dispersion viscosity. When coated with alcohol or glycerol, which have similar functional groups, no clear trend could be detected between the dispersion viscosity and the miscibility of the nanoTiO_2 particle. Moreover, the silanol-functionalized PVA formed a gel, which makes the results even more incomparable. The f-PVA-based dispersion viscosity measurements and electrospinning could not be carried out from the original solution but had to be done with diluted and filtered solution.

3.11 Production of PVA/nanoTiO_2 fiber networks by electrospinning

Fiber formation and fiber diameter are know to be tailorable by modifying the solution viscosity and electrospinning parameters (paper IV); high viscosity and low electrospinning field strength result in fibers, not spots, and a large fiber diameter. When the (dispersion) viscosity was too low, drops were formed instead of fibers, as with the f-PVA/nanoTiO_2 (Figure 12). The viscosities of the n-PVA- and a-PVA-based dispersions were similar, but the process parameters were different in these dispersions. The functional groups of the polymers and the coating agents seem to influence the interaction of the components and therefore the process parameters needed to be adjusted for each of the dispersions separately, because the aim was to produce a visible circular coating area on the substrate. The s-PVA-based fiber diameters and standard deviations varied (Figure 13) more than those of the n-PVA- and a-PVA-based fibers. It seems that the polymer properties (weight average molar mass and the molecular weigh distribution) resulted in a wide fiber diameter deviation due to the different miscibility behavior of the nanoTiO_2 particles phase during the polymerization phase.

All of the dispersions were able to carry the nanoTiO_2 particles with the polymer solution. The miscibility of the nanoTiO_2 particles correlated directly with their density along the electrospun fibers: the better the miscibility of the nanoTiO_2 particle during the emulsion polymerization, the higher their density was along the electrospun fibers. The coating agent of the nanoTiO_2 particles influenced the dispersion of the particles along the fibers. Some nanoTiO_2 agglomerates were found in all of the electrospun fibers, although, the nanoTiO_2 particles were coated to prevent agglomeration. As the miscibility of the particles increased from non-miscible to poorly miscible, the formation of the nanoTiO_2 agglomerates decreased. Agglomerates of the well-dispersed nanoTiO_2 (al) particles were found, too, which is an indication of an extensive

concentration of the filler. The visual appearances of the polymer beads and the nanoTiO_2 particle agglomerates were different. The polymer beads looked smooth in the SEM images where as agglomerated filler particles had rough surfaces. Polymer beads are know to form when the solution viscosity is not high enough for that specific system, and it could be concluded that the nanoTiO_2 particles did not change this phenomenon.

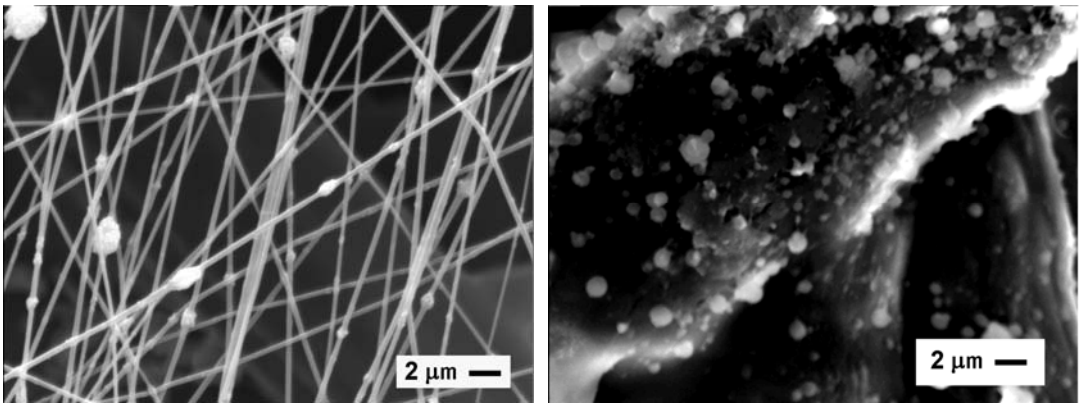

Figure 12. Typical SEM micrographs of PVA/nanoTiO_2 structures produced by electrospinning: non-modified PVA/nanoTiO_2 (gl) (left) and silanol functionallized PVA/nanoTiO_2 (gl) (right). NanoTiO_2 forms agglomerates, which appear as white gloss (reproduced from IV).

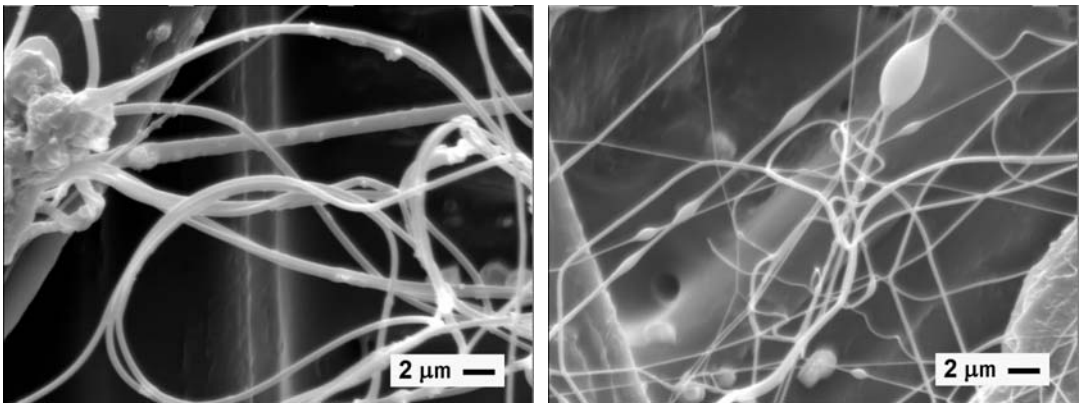

Figure 13. SEM micrographs of fibers of laboratory scale PVA with nanoTiO_2 (oh) (left) and nanoTiO_2 (gl) (right) produced by electrospinning. NanoTiO_2 forms agglomerates, which appear as white gloss (reproduced from IV).

Surface properties of the electrospun coated paper were studied more closely with a nanoTiO_2-filled fully hydrolyzed PVA solution. Some u-PVA-based preliminary tests, which are not published in any of the referred papers, were carried out to ensure a complete coverage of the electrospun fiber network coating. The coating appears smooth on the surface of the non-woven substrate, bur some defects are detected, eg. inward curled drops on the fiber network. NanoTiO_2

agglomerates were formed along the PVA fibers as presented in paper V, which could not be prevented by changing the feeding order of the components in the preparation of the dispersions, as was done with the PVA/clay-based dispersions.

The electrospun u-PVA/nanoTiO_2 (gl) fiber network coating seemed to seal the pores of the paper substrate, which influenced the ink penetration and the ink demand. As the polymer nanofiller fiber coating layer thickened with the coating time, the ink demand increased, as expected. The contact angle increased simultaneously with the coating time until an equilibrium was reached. A fully hydrolyzed poly(vinyl alcohol) is hydrophobic and therefore the electrospun coating increases the hydrophobicity of the coated surface. However, the hydrophilicity increased in our studies as the coating layer thickened and therefore it can be concluded that the hydrophilic nanoTiO_2 within the fibers influenced on the contact angle more than the hydrophobic polymer.

4 CONCLUSION

It can be challenging to prepare a homogenous polymer nanocomposite. In this work, polypropylene/nanoclay composites were prepared by melt processing and PVA/nanoclay, PVA/nanoTiO_2, and PA66/nanoclay fibers, in turn, were produced by electrospinning. Improved mechanical, flame retardant, and surface properties resulted from the addition of nanofillers.

Natural layered clay does not spontaneously disperse in polypropylene melt and therefore it was rendered more organic in nature with a novel amine, N-methylundecenylamine, and with octadecylamine. The cation exchanged clays enhanced the penetration of the metallocene catalyst hydroxyl-functionalized polypropylene compatibilizer, thus enabling the polypropylene matrix to penetrate between the intercalated clay sheets in melt blending. The partially exfoliated structure of the clay in the PP-based composites was achieved with the novel PP-*co*-OH compatibilizer and with a PP-*g*-MA compatibilizer.

The degree of exfoliated structure in a commercial modified clay was increased when ATH particles were added to the PP/clay nanocomposites due to the increased shear stress caused by the ATH particles. The ATH particles and the clay sheets seem to be competing for interactions with the compatibilizers, which resulted in a difference in the morphology of the PP/nanocomposites. The nanocomposites showed improved stiffness and reduced heat release rates but weakened toughness and increased moisture absorption relative to the unfilled PP or PP/clay composites.

A commercial grade PP aliphatic wax had a poor ability to widen the space between the clay layers and enhance a favorable interaction between the clay galleries and the PP chains. Intercalated or exfoliated clay structures were not achieved by melt blending in similar process conditions to those used when PP-*co*-OH and PP-*g*-MA were used as compatibilizers.

PVA and PA66 fibers with nanoscale diameters with nanoclay were produced by the electrospinning technique. The dispersions were able to carry the nanoclay from the nozzle to the substrate. The sizes of the clay particles were smaller within electrospun fibers when PVA and PA66 were polymerized in the presence of clay than when the components were prepared by mixing the components together in a suitable solvent.

The carboxyl groups along the PVA chains did not influence the fiber diameters and networks. The silanol-functional PVA, on the other hand, formed narrower and separate fibers, not networks. The feeding order of the nanoclay and the polymer had a major influence on the

dispersion viscosity, but to our surprise, the fiber networks were similar. This indicates that the viscosities were above the fiber forming limit and therefore, the differences in the viscosities had a modest influence on the fiber formation.

The PA66 with nanoclay formed a visually smooth and continuously coated circular area with a few separate spots on the substrate, except for one where the dispersion deposited completely isolated spots. The dispersion viscosities remained nearly constant in the dispersion conditions when the pH or the feeding order of the components was changed.

Finally, PVA/nanoTiO_2 dispersions were electrospun and all of the dispersions were able to carry the filler to the substrate. When the dispersions were prepared by mixing the components together, the fiber formation and the nanoparticle distribution were influenced by the carboxyl- and silanol-groups of the PVA and by changing the coating agent on the nanoTiO_2 particles. When the dispersions were prepared by synthesizing the vinyl monomer in the presence of the nanoTiO_2 particles, the miscibility of the filler particles influenced the filler distribution along the fibers. The PVA/nanoTiO_2 fiber network increased the hydrophobicity of a paper substrate.

References

1. Wypych, G., *Handbook of Fillers*, 2nd ed. Toronto: ChemTec Publishing, (1999).
2. Kawasumi, M., Hasegawa N., Kato, M., Usuki, A., Okada, A., Preparation and mechanical properties of polypropylene-clay hybrids, *Macromol.*, **300** (1997) 6333-6338.
3. Hasegawa, N., Kawasumi, M., Kato, M., Usuki, A., Okada, A., Preparation and mechanical properties of polypropylene-clay hybrids using a maleic anhydride-modified polypropylene oligomer, *J. Appl. Polym. Sci.*, **67** (1998) 87-92.
4. Bureau, M. N., Denault, J., Mechanical behavior and crack propagation in injection – molded polyamide6/clay nanocomposites, *Antec 2001 Conference proceedings*, **II** (2001) 2125-2129.
5. Svoboda, P., Zeng, C., Wang, H., Lee, L. J., Tomasko, D. L., Morphology and mechanical properties of polypropylene/organoclay nanocomposites, *J Appl Polym. Sci.*, **85** (2002) 1562-1570.
6. Zanetti M., Camino G., Reichrt P., Mülhaupt R., Thermal behavior of poly(propylene) layered silicate nanocomposites, *Macromol. Rapid Commun.*, **22 (**2001) 176-180.
7. Modesti, M., Lorenzetti, A., Bon, D., Besco, S., Thermal behavior of compatibilized polypropylene nanocomposite: effect on processing conditions, *Polym. Degr. Stab (2005) article in press*.
8. Gorrasi, G., Tortora, M., Vittoria, V., Kaempfer, D., Mülhaupt, R., Transport properties of organic vapors in nanocomposites of organophilic layered silicate and syndiotactic polypropylene, *Polymer*, **44** (2003) 3679-3685.
9. Osman, M. A., Atallah, A., *Macromol. Rapid Commun.* High-Density Polyethylene Micro- and Nanocomposites: Effect of Particle Shape, Size and Surface Treatment on Polymer Crystallinity and Gas Permeability **25** (2004) 1540-1544.
10. Hull, T.R., Price, D., Liu, Y., Wills, C.L., Brady J., An investigation onto the decomposition and burning behavior of ethylene-vinyl acetate copolymer nanocomposite materials, *Polym. Degr. Stab.*, **82** (2003) 365-371.
11. Qin, H., Zhang, S., Zhao, C., Hu, G., Yang, M., Flame retardant mechanism of polymer/clay nanocomposites based on polypropylene, *Polymer*, **46** (2005) 8386-8395.
12. Gilman, J. W., Jackson C. L., Morgan A. B., Harris Jr. R., Manias E., Giannelis E. P-. Wuthenow M., Hilton D., Phillips S. H., Flammability properties of polymer-layered-silicate

nanocomposites. Polypropylene and polystyrene nanocomposites, *Chem. Mater*., **12** (2000) 1866-1873.

13. Zanetti, M., Kashiwagi, T., Falqui, L., Camino, G., Cham. Cone calorimeter combustion and gasification studies of polymer layerd silicate nanocomposites, *Mater*., **14** (2002) 881-887.
14. Tang, Y., Hu, Y., Li, B., Liu, L., Wang, Z., Chen, Z., Fan, W., Polypropylene/montmorillonite nanocomposites and intumescent, flame-retardant monmorillonite synenergism in polypropylene nanocomposites, *J. Polym. Sci. Part A: Polym. Chem,* **42** (2004) 6163-6173.
15. Manias E., Touny A., Wu L., Strawhecker K., Lu B., Chung T.C., Polypropylene/montmorillonite nanocomposites; a review of synthetic routes and materials properties, *Chem. Mater*., **13** (2001) 3516-3523.
16. Hwang, W.-G., Wei, K.-H., Wu, C.-M., Mechanical, thermal, and barrier properties of NBR/organosilicate nanocomposites, *Polym. Eng. Sci*. **44** (2004),11, 2117-2124.
17. Nabok, A., Organic and Inorganic Nanostructures, Nanotechnology series, Artch House, New York (2005) pp. 260.
18. Garces, J. M., Moll, D. J., Bicerano, J., Fibiger, R., McLeod, D. G., Polymeric nanocomposites for automotive applications, *Advanced Mater.* **12** (2000) 23, 1835-1839.
19. Tsukruk, V. V., Molecular lubricants and glues for micro- and nanodivices, *Advanced Mater*. **13** (2001) 2, 95-108.
20. Markarian, J., Automotive and packaging offer growth opportunities for nanocomposites, *Plastics Additives and Compounding* **7** (2005) 6, 18-21.
21. Presting, H., König, U., Future nanotechnology developments for automotive applications, *Mater. Sci. Eng. C* **23** (2003) 737-741.
22. Gao, F., Beyer G., Yuan, Q., A mechanistic study of fire retardancy of carbon nanotube/ethylene vinyl acetate copolymers and their clay composites, *Polym. Deg. Stab*. **89** (2005) 559-564.
23. Drew, C., Bruno, F. F., Wang, X., Ku, B.-C., Samuelson, L. A., Kumar J., Electrostatic layer-by-layer assembly on polyelectrolytes on surface functionalized electrospun nanofibers and metal oxide deposition, *Polymeric Mater: Sci. Eng.* **91** (2004) 945-946.
24. Drew, C., Wang, X., Senecal, K., Schreuder-Gibson, H., He, J., Tripathy, S., Samuelson, L., Electrospun nanofibers of electronic and photonic polymer systems, *ANTEC 58th* , **2** (2000) 1477-1481.

25. Kim, H. S., Sung, J. H., Choi, H. J., Cin, I.-J., Jin, H.-J., Electrospun nanofiber of multi-walled carbon nanotube and poly(methyl methacrylate) composites, *Polymer Preprints*, **46** (2005) 2, 736-737.
26. Hambir, S., Bulakh, N., Jog, J.P., Polypropylene/clay nanocomposites: effect of compatibilizer on the thermal, crystallization and dynamic mechanical behavior, *Polym. Eng. Sci.*, **42** (2002) 9, 1800-1807.
27. Jayraman, K., Maechant, D., Rheological probing of structure in polypropylene/clay nanocomposites, *Antec* (2001) 654.
28. Wang, K. H., Choi, M. H., Koo, C. M., Xu, M., Chung, I. J., Jang, M. C., Choi, S. W., Song, H. H., Morphology and physical properties of polyethylene/silicate nanocomposite prepared by melt intercalation, *J. Polym Sci. Part B: Polym. Phys*., **40** (2002) 1454-1463.
29. Lu, C., Mai, Y.-W., Influence of aspect ratio on barrier properties of polymer –clay nanocomposites, *PRL*, **95** (2005) 088303-1-4.
30. Rahma, F., Fellahi, S., Performance evaluation of synthesized acrylic acid grafted polypropylene with $CaCO_3$/polyprolypele composites, *Polym. Comp.* **21** (2000) 175-186.
31. Jancar, J., Kucera, J., Yield behavior of PP/$CaCO_3$ and PP($Mg(OH)_2$ composites, II: Enhanced interfacial adhesion, *Polym. Eng. Sci.,* **30** (1990) 714-720.
32. Alexandre M., Dubois P., Polymer-layered silicate nanocomposites: preparation, properties and used of a new class of materials, *Mater. Sci. Eng*., **28** (2000) 1-63.
33. Nakajima, H., Yamada, K., Iseki, Y., Hosada, S., Hanai, A., Oumi, Y., Teranishi, T., Sano, T., Preparation and characterization of polypropylene/mesoporous silica nanocomposites with confined polypropylene, *J. Polym. Sci. Part B: Polym. Phys.* **41** (2003) 3324-3332.
34. Yang, F., Zhang, X., Zhao, H., Chen, B., Huang, B., Feng, Z., Preparation and properties of polyethylene/montmorillonite nanocomposites by *in situ* polymerization, *J. Appl. Polym. Sci*., **89** (2003) 3680-3684**.**
35. Salem, N., Shipp, D. A., Polymer-layered silicate nanocomposite prepared though in situ reversible addition-fragmentation chain transfer (RAFT) polymerization, Polymer, **36** (2005) 8573-8581.
36. Hornsby, P. R., Cusack, P. A., Cross, M., Toth, A., Zelei, B., Marosi, G., Zink hydroxystannate-coated metal hydroxide fire retardants: fire performance and substrate-coating interactions, *J. Mater. Sci.*, **38** (2003) 2893-2899.

37. Bureau, M. N., Perrin-Sarizin, R., Ton-That, M.-T., Polyolefin nanocomposites: essential work of fracture analysis, *Polym. Eng. Sci*., **44** (2004) 6, 1142-1151.
38. Lee, E. C., Mielewski, D. F., Baird, R. Exfoliation and dispersion enhancement in polypropylene nanocomposites by in-situ melt phase ultrasoication, *J., Polym. Eng. Sci.,* **44** (2004) 9, 1773-1781.
39. Kawasumi, M., Hasegawa N., Kato, M., Usuki, A., Okada, A., Preparation and mechanical properties of polypropylene-clay hybrids, *Macromol.*, **300** (1997) 6333-6338.
40. Zilg, C., Thomann, R., Baumert, M., Finter, J., Mulhaupt, R., Nanocomposites auf Schichtsilikatbasis, *Macromol. Rapid Commun*., **21** (2000) 17, 1214-1219.
41. Reichert P., Nizt H., Klinke S., Brandsch R., Thomann R., Mülhaupt R., Poly(propylene)/organoclay nanocomposite formation: influence of compatibilizer functionality and organoclay modification, *Macromol. Mater. Eng*. **275** (2000) 8-17.
42. Liu, X., Wu, Q., PP/clay nanocomposites prepared by grafting-melt intercalation, *Polymer*, **42** (2001) 10013-10019.
43. Plummer, S. J. G., Garamszeni L., Leterrier, Y., Rodlenr M., Månson J.-A. E., Hyberbranced polymer layered silicate nanocomposites, *Chem. Mater.*, **14** (2002) 486-488.
44. Shah R. K., Paul, D. R., Surlyn ionomer based nanocomposites by melt processing: the role of alkyl tails on exfoliation, *Polym. Mat. Sci. Eng*., **91** (2004) 982-983.
45. Le Pluart, L., Duchet J., Sautereau, H., Gerard, J. F., Tailored interfaces in nanocomposites, *Macromol. Symp.*, **194** (2003) 155-160.
46. Odian, G., Principles of Polymerization, 3 ed. New York, (1991) p. 747.
47. Finch, C. A., Industrial Water Soluble Polymers, Cornwall, The Royal Society of Chemistry (1996) p. 160.
48. Kim., Y., White, J. L., Melt-Intercalation Nanocomposites with Chlorinated Polymers, *J. Appl. Polym. Sci.*, **90** (2003) 1581-1588.
49. Lew, C.Y., Murphy, W. R., McNally, G. M., Preparation and properties of polyolefin-clay nanocomposites, *Polym. Eng. Sci*., **44** (2004) 6, 1027-1035.
50. Ryul, J. G., Lee, P. S., Kim, H. S., Lee, J. K., Development of PP-based nanocomposites via in-situ copolymerization and melt intercalation with the power ultrasonic wave, *Antec* (2001) 2136-2139.

51. Drew C., Ku, B.-C., Wang, X., Samuelson, L. A., Kumar, J., Electrostatic assembly of titanium dioxide on surface functionalized electrospun nanofibers, *Polymer Preprints,* **44** (2003) 2, 111.
52. Seymor, R., Carraher, C. E., Structure-Property Relationships in Polymer, (1984) Plentum Press, New York, pp. 219.
53. Liu, X., Wu, Q, Polyamide 66/Clay nanocomposites via melt intercalation, *Macromol. Mater. Eng.*, **287** (2002) 180-186.
54. Zhang, L.-F., Guo, B.-H., Zhang, Z.-M., Synthesis of multifunctional polypropylene via solid phase cografting and its grafting mechanism, *J. Appl. Polym. Sci*, **84** (2002) 929-935.
55. Villar, M. A.,Ferreira, M.L., Co- and terpolymerization of ethylene, propylene, and higher α-olefins with high polypropylene contents using metallocene catalyst, *J. Polym. Sci.: Part A: Polym Chem.*, **39** (2001) 7, 1136-1148.
56. Datta H., Singha, N. K., Bhowmick A. K., Beneficial effect of nanoclay in atom transfer radical polymerization of ethyl acrylate: a one pot preparation of tailor-made polymer nanocomposite, *Macromol.*, **41** (2008) 1, 50-57.
57. Rong, M. S., Zhang, M. Q., Pan, S. L., Lehmann B., Friedrich, K., Analysis of the interfacial interactions in polypropylene/silica nanocomposites, *Polym. Int*., **53** (2004) 176-183.
58. Xie S., Zhang, S., Wang, F., Synthesis and characterization of poly(propylene)/montmorillonite nanocomposites by simultaneous grafting-intercalation, *J. Appl. Polym. Sci.*, **94** (2004) 1018-1023.
59. T. F. McKenna, J. B. P. Soares, and L. C. Simon, Polyfin reaction engineering – an overview of recent developments, *Macromol. Mater. Eng.*, **290** (2005) 507-510
60. Dubois P., Alexandre, M., Jerome, R., Polymerization-filled composites and nanocomposites by coordination catalysis, *Macromol. Symp.*, **194** (2003) 13-26.
61. Chung T. C., Metallocene-mediated synthesis of chain-end functioinalized polypropylene and application in PP/clay nanocomposites, *J. Organ. Chem.* **690** (2005) 6292-9299.
62. Wang Z., Chung, T. C., Synthesis on chain-end functionalized polypropylene and its applications in exfoliated PP/clay nanocomposite, *Polym. Mater. Sci. Eng.*, **93** (2005) 573.
63. Wang, W.-J., Cin, W.-K., Wang, W.-J., Synthesis and structural characterization of [chromophore]$^{+}$ -saponite/polyurethane nanocomposites, *J. Polym. Sci., Part B: Polym Phys*., **40** (2002) 1690-1703.

64. Kato, M., Usuki, A., Okada, A., Synthesis of polypropylene oligomer - clay intercalation compounds, *J. Appl. Polym. Sci.,* **66** (1997) 1781-1785.
65. Suh, I. S., Ruy, S. H., Bae, J. H., Chang, Y. W., Effects of compatibilizer on the layered silicate/ethylene vinyl acetate nanocomposite, *J. Appl. Polym. Sci.*, **94** (2004) 1057.
66. Mehrabzadeh, M., Kamal, M. R., Melt processing of PA66/clay, HDPE/clay and HDPE/PA66/clay nanocomposites, *Po. Eng. Sci*., **44** (2004) 6, 1152-1161.
67. Li, J., Zhou, C., Wang, G., Zhao, D., Study of rheological bejhavior of polypropylene/clay nanocomposites, *J. Appl. Polym. Sci,,* **89** (2003) 3609-3617.
68. Bureau, M. N., Perrin-Sarizin, R., Ton-That, M.-T., Polyolefin nanocomposites: essential work of fracture analysis, *Polym. Eng. Sci*., **44** (2004) 6, 1142-1151.
69. Lee, E. C., Mielewski, D. F., Baird, R. J., Ultrasonic oscillations induced morphology and property development of polypropylene/montmorillonite nanocomposites, *Polym. Eng. Sci*., **44** (2004) 9, 1773-1781.
70. Chang, Y. W., Yang, Y., Ryu, S., Nah, C., Preparation and properties of EPDM/organomontmorillonite hybrid nanocomposites, *Polym. Int*. **51** (2002) 319-324.
71. Liang, J.-Z., Melt rheology of nanometer-calcium-carbonate-filled acrylonitrile-butadiene-styrene (ABS) copolymer comosites during capillary extrusion, *Polym. Int*., **51** (2002) 1473-1478.
72. Ton-That, M.-T., Perrin-Sarazin, E., Cole, K.C., Bureau, M.N., Denault, J., Polyolefin formulation and development, *Polym. Eng. Sci.,* **44** (2004) 7, 1212-1219.
73. Ogata, N., Kawakage, S., Ogihara, T., Poly(vinyl alcohol)- clay and poly(ethylene oxide)-clay blends using water a solvent, *J. Appl. Polym. Sci.*, **66** (1997) 573-581.
74. Pourabas, B., Raeesi V., Preparation of ABS/ montmorillonite nanocomposite using a solvent/non-solvent method, *Polymer*, **46** (2005) 5533-5540.
75. Yeh, J.-M., Liou, S.-J., Lai, M.-C., Chang, Y.-W., Huang, C.-Y., Chen, C.-P., Jaw, J.-H., Tsai, T.-Y., Yu, Y.-H., Comparative studies of the properties of poly(methyl methacrylate)-clay nanocomposite material prepared by *in situ* emulsion polymerization and solution dispersion, *J. Appl Polym. Sci*., **94** (2004) 1936-1946.
76. Yu, T., Lin, J., Xu, J., Chen, T., Lin, S., Novel polyacrolonitrile nanocomposites containein Na-montmorillonite and nano SiO_2 particle, *Polymer* **46** (2005) 5695-5697.

77. Xie, W., Hwu, J. M., Jiang, G. J., Buthelizi T. M., Pan, W.-P., A study of the effect of surfactants on the properties of polystyrene-montmorillonite nanocomposites, *Polym. Eng. Sci.*, **43** (2003) 1, 214-222.
78. Chibowsky, S., Paskiwich, M., Studies of the influence of acetate groups from polyvinyl alcohol on adsorption and electrochemical properties of the TiO_2- polymer solution interface, *J. Disp. Sci. Technol.*, **22** (2001) 2&3, 281-289.
79. Gedde, U. W., Polymer Physics, London, Chapman Hall (1995) p. 292.
80. Ham, G. E., Vinyl polymerization, Volume 1, New York, Mercel Dekker, Inc., (1967), p. 509.
81. Doshi J, Reneker J., Electrospinning process and application of electrospun fibers, *Electrostatics*, **35** (1995) 151-160.
82. Shao, C, Kim, H.-Y., Gong, J., Ding, B., Lee, D.-R., Park, S.-J., Fiber mats of poly(vinyl alcohol)/silica composite via electrospinning, *Materials, Letters*, **57** (2003) 1579-1584.
83. Sanders, E. H., Kloefkorn, R., Bowlin, G. L., Simpson, D. G., Wnek, G., E., Two phase electrospinning from a single electrified jet: microencapsulation of aqueous reservoirs in poly(ethylene-*co*-vinyl acetate) fibers, *Macromolecules*, **36** (2003) 11, 3803-3805.
84. Angels, M., Cheng, H.-L., Venkar, S. S., Emulsion electrospinning: composite fibers from drop breakup during electrospinning, *Pol. Adv. Tech*., (2007) on line Dec 17th.
85. Shenoy, S. L., Bates, W. D., Frisch H., L., Wnek G. E., Role of chain entanglements on fiber formation during electrospinning of polymer solutions: good solvent, non-specific polymer-polymer interaction limit, *Polymer*, **46** (2005) 3372-3384.
86. Drew C., Wang, X., Samuelson L. A., Kumar, J., The Effect of Viscosity and Filler on Electrospun Fiber Morphology, *J. macromol. Sci. Part A- Pure and Appl. Chem.*, **12** (2003) A40, 1415-1422.
87. Fong, H., Chun, I., Reneker, D. H., Beaded nanofibers formed during electrospinning, *Polymer*, **40** (1999) 4585-4592.
88. Smit, E., Buttner, U., Sanderson, R.D., Continous yarn from electroslun fibers, *Pol. Comm*., **46** (2005) 2419-423.
89. Zong, X., Kim, K., Fang, D., Ran, S., Hsiao, B. S., Chu, B., Structure and process relationship of electrospun bioabsorbable nanofiber membranes, *Polymer*, **43** (2002) 4403-4412.

90. Tan, S.H., Inai, R., Kotaki, M., Ramakrishna, S., Systematic parameter study for ultra-fine fiber fabrication via electrospinning process, *Polymer*, **46** (2005) 6128-6134.
91. Lee, J. S., Choi, K. H., Ghim, H. D., Kim, S. S., Chun, D. H., Kim, H., Y., Lyoo W. S., Role of molecular weight of atactic poly(vinyl alcohol) (PVA) in the structure and properties of PVA nanofabric prepared by electrospinning, *J. Appl. Polym. Sci*., **93** (2004) 1638-1646.
92. McKee, M. G., Long, T. E., Implication of hydrogen bonding on rheological/electrospinning relationships, *Polymer* **24** (2004) 2, 130-131.
93. Deitzel, J. M., Kosik. W., McKnight, S. H., Beck Tan, N.C., DeSimone, J.M., Crette, S., Electrospinning of polymer nanofibers with specific surface chemistry, *Polymer*, **43** (2002) 1025-1029.
94. Li, L., Hsieh, Y.-L., Ultra-fine polyelectrolyte fibers form electrospinning of poly(acrylic acid), *Polymer*, **46** (2005) 5133-5139.
95. Wutticharoenmongkol, P., Sandhavanakit, N., Pavasant, P., Supaphol, P., Preparating and characterization of novel bone scaffolds based on electrospun polycaprolactone fibers filled with nanoparticles, *Macromol. Biosci.*, **6** (2006) 70-77.
96. Jeong, J., S., Moon, J. S., Jeon S. Y., Park, J. H., Alegaonkar, P. S., Yoo, J. B., Mechanical properties of electrospun PVA/MWNTs composites nanofibers, *Thin Solid films*, **515** (2007) 5136-5141.
97. Mo, X.M., Xu, C. Y., Kotaki, M., Ramakrishna, S., Electrospun P(LLA-CL) nanofiber: a biomimetic extracellular matrix for smooth muscle cell and endothelia cell proliferation, *Biomaterials*, **25** (2004) 1883-1890.
98. Buchko, C. J., Chen, L. C., Shen, Y., Martin, D. C., Processing and microstructural characterization of porous biocompatible protein polymer thin films, *Polymer*, **40** (1999) 7397-7407.
99. Kidoaki, S., Kwon, K., Matsuda, T., Mesoscopic spatial designs of nano- and microfiber meshes for tissue-engineering matrix and scaffold based on newly devised multilayering and mixing electrospinning techniques, *Biomaterials*, **26** (2005) 37-46.
100. Hakala, K., Helaja, T., Löfgren, B., Metallocene/Methylaluminoxane-Catalyzed Copolymerizations of Oxygen-Functionalized Long-Chain Olefins with Ethylene, *J. Polym. Sci., Part A: Pol. Chem*., **38** (2000) 1966- 1971.
101. Heikkilä, Pirjo, Nanostructured Fibre Composites, and Materials for Air Filtration, Tampere University of Technology, 2008, Publication 749.

102. Huang, T. C.; Toraya, H.; Blanton, T.N.; Wu, Y., X-ray powder diffraction analysis of silver behenate, a possible low-angle diffraction standard, *J. Appl. Crystallogr*., **26 (**1993) 180–184.
103. ASTM E104-51 (Reappr. 1971), Standard Recommended Practice for Maintaining Constant Relative Humidity by Means of Aqueous Solutions, *Annual Book of ASTM Standards 08.03 Plastics (III)*, Am. Soc. Testing and Materials, Philadelphia PA 1984, p 609-612
104. Boyed R.H, Phillips P. J., The Science of Polymer Molecules, Cambridge Solid State Science Series, 1993
105. Trodjeman, Ph. Robert, C., Marin, G., Gerard, P., The effect of α, β crystalline structure on the mechanical properties of polypropylene, *Eur. Phys. J. E.*, **4** (2001) 459-465.
106. Karger-Kocsis, J., How does phase transformation work with semicrystalline polymers, *Polym. Eng. Sci.*, **36** (1996) 2, 203-210.
107. Lipponen, S., Pietikäinen, P., Vainio, U., Serimaa, R., Seppälä J., Silane functionalized ethylene/diene copolymer modifiers in composites of heterophasic polypropylene and microsilica, *Polym. Polym. Comp*., **15** (2007) 5, 343-355.
108. Zhen, W., Lu, X., Toh, C. L., Zhen. T. H., He, C., Effects of clay on polymorphism of polypropylene in polypropylene/clay nanocomposites, *J. Polym. Sci: Part B.*, **42** (2004) 10, 1810-1816.
109. Saujanya C., Radhakrishnan S., Structure development and crystallization behavior of PP/nanoparticulate composite, *Polymer*, **42** (2001) 16, 6723-6731.
110. Garcia-Martinez J.M., Laguna O., Areso S., Collar E. P., Polypropylene/mica composites modified by succinic anhydrice-grafted atactic polypropylene: a thermal and mechanical study under dynamic conditions, *J. Appl. Pol. Sci.*, **81** (2001) 3, 625-636.
111. Gianelli, W., Ferrara, G., Camino, G., Pellegatti, G., Roesnthal, J., Trombin, R.C., Effect of matrix features on polypropylene layered silicate nanocomposites, *Polymer*, **46** (2005) 18, 7037-7046.
112. Powell, P. C., Engineering with Polymers, Chapman and Hall, London, 1983, p. 312
113. Kulichikhin, V.G., Tsamalashvili, L.A., Plotnikova, E.P., Barannikov, A.A., Kerber, M.L., Fischer, H., Rheological properties of liquid precursors of polypropylene-clay nanocomposites, *Pol. Sci. Ser. A.*, **45** (2003) 6, 564-572.

114 Misra, S., Naik, J. B., Absorption of water at ambient temperature and steam in wood-polymer composites prepared from agrowaste and polystyrene, *J. Appl. Polym. Sci*., **68** (1998) 681-686.

115 Rozman, H. Z., Kumar, R. N., Abusamah Addl, M. R., Mohd Ishak, Z. A., The Effect of Lignin and Surface Activation on the Mechanical Properties of Rubberwood-Polypropylene composites, *J. Wood Chem. Technol*. **18** (1998) 471-490.

116. Lehtinen T, Sundholm G, Holmberg S, Sundholm F, Bjormbom P and Bursell M, Electrochemical characterization of PVDF-based proton conduction membranes for fuel cells, *Electrochem Actai,* **43** (1998) 1881-1890.

ISBN 978-951-22-9895-2
ISBN 978-951-22-9896-9 (PDF)
ISSN 1795-2239
ISSN 1795-4584 (PDF)